National University of Science and Technology POLITEHNICA Bucharest

Doctoral School of Aerospace Engineering

Engineering Sciences, Aerospace Engineering

DOCTOR OF PHILOSOPHY THESIS

extended abstract

Numerical and experimental contributions on perforated plate passive flow control technique applied to vaned diffusers for microgas turbines

PhD Candidate: **Eng. Mihnea Gall**

PhD Supervisor: **Prof. dr. eng. Daniel-Eugeniu Crunțeanu**

Bucharest, 2025

National University of Science and Technology POLITEHNICA Bucharest

Doctoral School of Aerospace Engineering

Engineering Sciences, Aerospace Engineering

DOCTOR OF PHILOSOPHY THESIS

extended abstract

Numerical and experimental contributions on perforated plate passive flow control technique applied to vaned diffusers for microgas turbines

PhD Candidate: **Eng. Mihnea Gall**

PhD Supervisor: **Prof. dr. eng. Daniel-Eugeniu Crunțeanu**

PhD evaluation board

President	Prof. dr. eng. Teodor Lucian Grigorie	National University of Science and Technology POLITEHNICA Bucharest
PhD Supervisor	Prof. dr. eng. Daniel-Eugeniu Crunțeanu	National University of Science and Technology POLITEHNICA Bucharest
Referent		
Referent		
Referent		

Bucharest, 2025

TABLE OF CONTENTS

LIST OF FIGURES

CHAPTER 1 MOTIVATION AND THESIS OBJECTIVES

1.1 Microgas turbines market analysis

In recent decades, considerable research has focused on microgas turbine engines (MGTs), aiming to discover game changing design features that can lead to enhanced performance. Growing concerns about greenhouse gas emissions have prompted countries around the world to implement stringent regulations aimed at producing energy with lower and lower environmental impact. In Europe, the successful implementation of the Green Deal is planning to achieve almost null net greenhouse gases emissions by 2050 [1]. With these worldwide strategies, the MGT market is anticipated to be propelled with more than $35 million by 2030, compared to the $26 million reported figure in 2021 [2]. The target applications for MGTs are often selected based on their high energy and power density characteristics which are requested by customers in the unmanned aerial vehicles market (UAV) or in the small-scale power generation industry [3].

With recent technological advancement for batteries and fuel cells, the MGTs must possess several features that make them desirable for end users, from financial and operational standpoints. The MGTs have proved flexibility and reliability in the operating environments. However, one of the main advantages reported in the literature for MGTs is the high energy density potential [4]. With reduced overall system efficiency, the power to weight ratio for a gas turbine engine is still higher compared to the battery technology existing nowadays, as it is also depicted in Figure 1-1. Even if hydrogen shows the highest energy density, its implementation in MGTs is still an active field of research, mainly due to its low density (and the need to use it as a cryogenic to reduce the system volume, especially for airborne applications) and safety considerations. Along with the energy density, the MGTs also show a higher power density compared to batteries as it is also summarized in Figure 1-2.

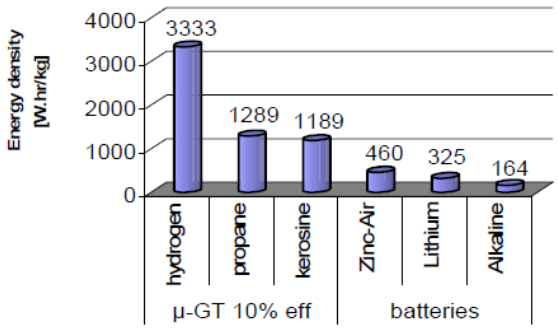

Figure 1-1 MGTs vs batteries energy density comparison [4]

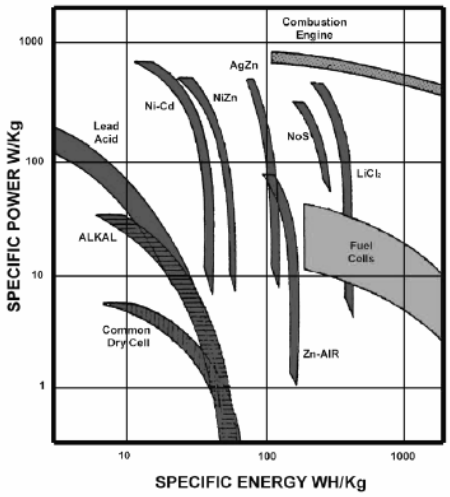

Figure 1-2 Specific power comparison [4]

Similar to large gas turbine engines, the MGTs are composed of five stages (Figure 1-3): inlet, compressor, combustor, turbine and nozzle. Typically, MGTs are designed with single stage radial or mixed flow centrifugal compressors as they are characterized by shorter length, lower cost, and simplified design compared to axial compressors. Additionally, centrifugal compressors are capable to achieve a higher pressure ratio in single stage configuration and they exhibit a broader operating range, characterized by flatter operating curves. They also demonstrate greater resilience to the impact of foreign objects, contributing to increased reliability and extended service life [6]. Furthermore, centrifugal stages demonstrate improved tolerance to distortions or irregularities in the incoming air flow.

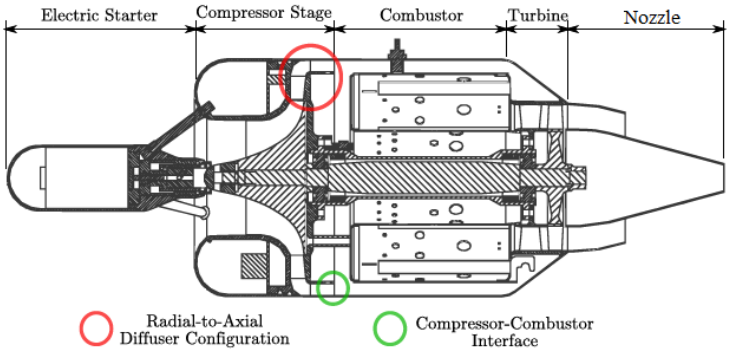

Figure 1-3 BMT120KS engine configuration [5]

Traditionally, a centrifugal compressor stage employed in MGTs has the following components from inlet to outlet: an impeller, a small vaneless diffuser, a radial diffuser, a 90° vaneless bend and an axial cascade with de-swirling purposes (Figure 1-4). The MGTs frontal area constraints directly impact the diameter of MGTs compressors which might limit their performance, especially in the diffuser part. To achieve high diffusion levels, compact and efficient diffusers are needed, as radial extension is limited by the above-mentioned frontal area constraints. The compression systems for airborne applications such as UAVs require high pressure ratio, high efficiency, reduced frontal diameter and reduced weight and complexity. As these requirements are conflicting, research efforts are needed to advance the technological level of novel highly competitive compression systems for MGTs.

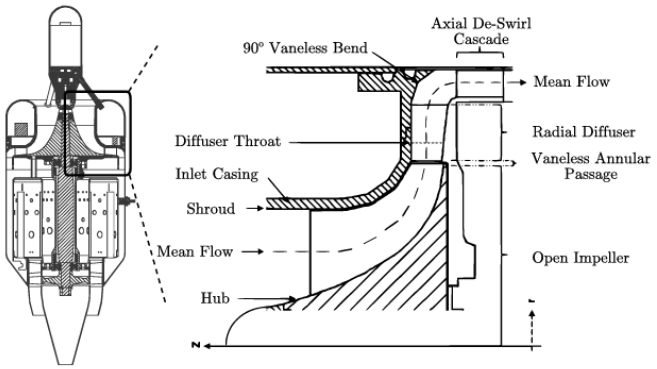

Figure 1-4 Classic centrifugal compressor stage for MGTs [5]

1.2 Flow control methods

Centrifugal compressors'performance is often evaluated in terms of total-to-total pressure ratio, total-to-static pressure ratio, isentropic efficiency or operating range. Depending on the specific application, the relative weight of these criteria is different leading to an optimal solution. In general, for high compression ration stages and high efficiency, vaned diffusers are employed within centrifugal stages. However, the vaned diffusers limit the stable operating range in contrast with the vaneless counterparts, which are less performant, but they suffer less from the above-mentioned disadvantage. Thus, the development of aerodynamic instabilities in the vaned diffusers at low flow rates, or the choke inception at high flow rates strongly limit the stable operating range of a centrifugal compressor stage and careful actions must be taken to mitigate their effects.

The stable operating range limitation is also affected by complex flow phenomena such as shock waves, boundary layer detachment, shock wave – boundary layer interaction (SBLI), tip flow losses or secondary flows. Tiainen [7] performed a comparative study between different active and passive control methods to improve the stable operating range. Different active or passive control features are found in the literature which consists of perforated or porous materials either on the hub or the shroud of the vaned diffuser with the final goal to extend the operating range, especially concentrating on the low flow rates regimes. Skoch [8] investigated an active method based on vaned diffuser hub air injection, using different injection angles of the injection holes (these were placed upstream of the vanes leading edge). The results showed a stall regime improvement using low injection flow rates or even zero injection corresponding to a passive solution. Galloway [9][10] studied the possibility to recirculate the fluid in the vaned diffuser by means of different cavity configurations (either independent cavities for each channel or common cavities for the entire vaned diffuser) either on the hub surface or on the shroud. With the hub recirculation strategy, a 58% increase in the stable operating range for high compression ratios was achieved.

The stable operating range limitation at high flow rates, namely choke, is associated with the shock waves, as well as with their interaction with the boundary layer. The boundary layer detachment as a result of the interaction with the shock waves additionally limits the effective flow area, with leads to a quicker choke. Moreover, the shock waves together with their interaction with the boundary layer are fully responsible for total pressure losses. The methods to increase the performance in this high flow rates regimes are linked to the shock waves intensity reduction by changes in shock type and structure, with the final goal to limit thier influence on the boundary layer and eventually to unchoke the flow channel. In the scientific literature, different studies tried to alter the shock waves configuration. These studies were first performed on external aerodynamics [11] (i.e. isolated airfoils) and subsequently on inlets [12], nozzles [13] and shock tubes [14].

Lee [15] shows a couple of methods for passive control of the shock waves induced oscillations for the flow past an airfoil (Figure 1-5). These methods are based on a common cavity placed underneath a porous/perforated material that allows a flow recirculation [16]. Thereby, the static pressure increase downstream the shock wave leads to a suction towards the cavity region and to a subsequent injection upstream the shock wave. Thus, a viscous ramp effect is created that allows for an oblique leading shock wave to be formed. A tiny normal trailing shock is still present which intersects the oblique one in the so called 'triple point'.

Compared to the initial single normal shock wave, the new oblique 'λ-type' shock structure is characterized by smaller intensity, reduced wave induced total pressure losses and remissive effect on shock induced separation of the boundary layer (Figure 1-6) [17]. Experimentally, the presence of the 'λ-type' shock structure is confirmed by a plateau in the wall static pressure distribution corresponding to the control region. The suction downstream the shock wave, caused by the introdution of the cavity, has also the goal to keep the flow attached [18][19]. Overall, the flow recirculation inside the cavity, not only changes the structure of the initial strong normal shock wave, but it also shifts its position, with the shock system starting position coinciding with the control region leading edge [20]. However, the blowing effect from the cavity affects the boundary layer leading to larger displacement and momentum thicknesses, especially in the rear part of the control region. The distortion in the velocity profiles also leads to a rise in the flow turbulence level.

A common understanding arises, namely the cavity dimensions needs to be optimized so that the suction and the fluid injection back into the main flow to be optimum, without an excessive boundary layer thicknening (Figure 1-7). A parametric study might take into account the cavity dimension (depth, length [21]), the relative position of the cavity to the initial shock wave attachment point, as well as the porosity factor dictated by the orifice size and gap in between. Recommendations from previous studies restrict the perforated plate control region length to 70 mm [22] to limit the so-called excrescence drag introduced by the holes. The orifice inclination was also studied, with the first half of the control region accommodating 30º or 45º inclined holes either forward or backward facing. For the second part of the perforated plate, normal to surface holes were employed [22]. Less disturbances and fuller velocity profiles were reported for the inclined orifices. Drag reduction was achieved for a circular arc half airfoil using forward facing orifies with 1-2% porosity [23].

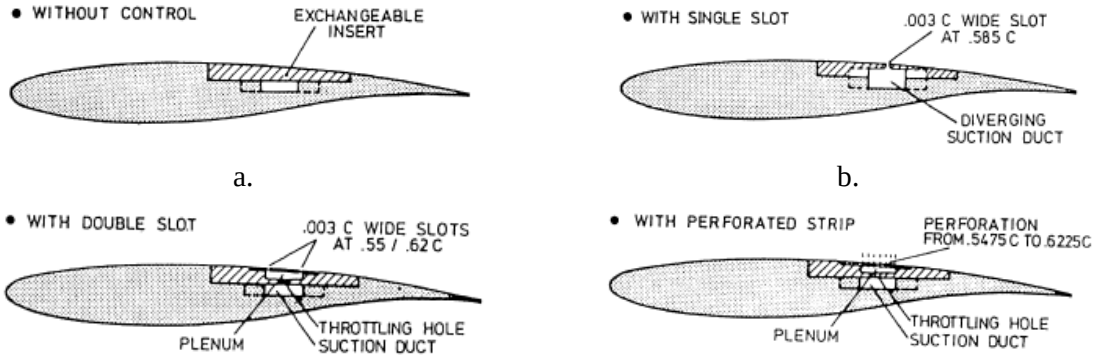

Figure 1-5 Passive control methods of shock waves on airfoils [15]

a. Reference airfoil b. Single slot airfoil c. Double slot airfoil d. Perforated strip airfoil

A notable influence of the porosity ratio and the length of the porous zone was reported in the literature to affect the so called 'λ-type' structure of the shock waves. An increase in the porosity factor leads to an increase in the viscous losses too. The skin friction of a perforated control region is at least twice the skin friction of a bare smooth wall. Thus, the reduction in total pressure losses by switching the normal shocks into oblique shocks, might be cancelled. or even exceeded by the additional viscous losses in case the perforated area geometry is not optimally implemented [24]. The increased viscous losses due to additional roughness introduced by the perforated plate orifices and cavity blowing, strongly limit the positive effect

of the perforated plate passive control strategy on the overall drag reduction. However, this passive control concept could still be of interest in applications such as supersonic intakes or turbomachinery components, where avoidance of shock induced separation is the main goal.

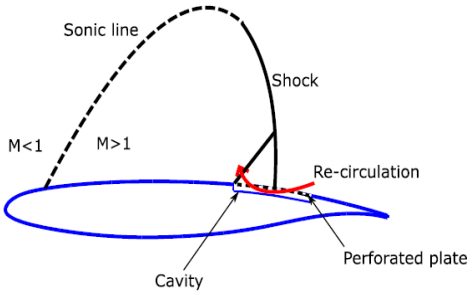

Figure 1-6 Shock wave passive control method – sketch [17]

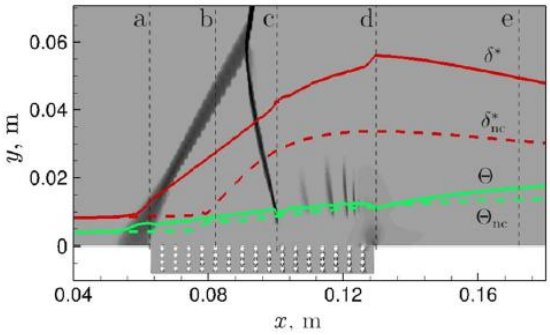

Figure 1-7 Boundary layer displacements [17] (green – reference, red – passive porous)

Experimentally, by means of Schlieren visualization, Savu et. al. [25] proved that a perforated airfoil might reduce the shock wave intensity, which overall leads to the reduction in total pressure losses and to the noise level reduction. This effect was achieved by employing a cavity similar to the one sketched in Figure 1-8 where a recirculation zone develops inside the cavity. Numerical and experimental results (Figure 1-9) for a perforated control region placed on nozzle walls are presented by Szulc [26]. Both the numerical simulations and the Schlieren visualization from the experiments show the perforated material ability to reduce the shock wave intensity by switching to a λ-type shock structure.

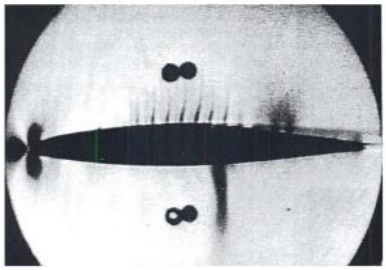

a. Schlieren image M = 0,785

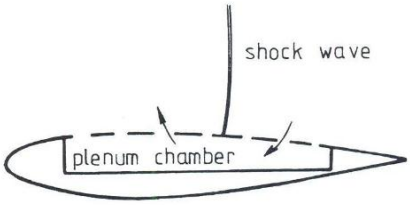

b. Airfoil porous surface concept

Figure 1-8 Shock waves passive control method [25]

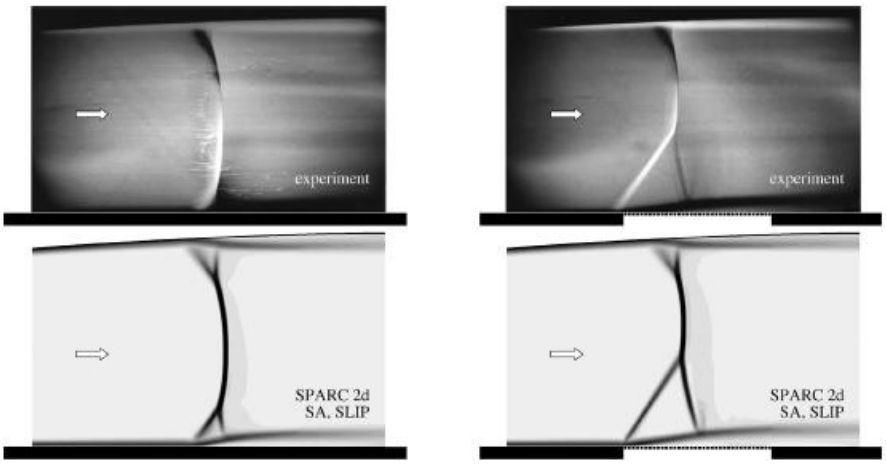

Figure 1-9 Numerical vs experimental results-nozzle flow [26] (smooth wall vs porous wall)

1.3 Thesis objectives

The main objective of the current thesis is to develop a new vane configuration for a microgas turbine centrifugal compressor vaned diffuser, characterized by the presence of a perforated plate passive control region with hollow cavity underneath that allows a flow recirculation to mitigate shock wave induced phenomena. By reducing the shock intensity at high flow rate off-design points, the passive control method is expected to increase the operating range of the vaned diffuser. Rather than limiting the application of perforated plates to single airfoils or internal walls (i.e. for nozzles, intakes), the current work focuses on the behaviour of perforated plates in cascade environments and the way they alter the shock waves structures. This confers the novel and genuine approach of this research as it extends the implementations of perforated plates to cascade arrangements, rather than limiting their use to single airfoils or bladeless internal flows. The successful implementation of the proposed new vane configuration, followed by subsequent technological readiness level advancement might lead to large scale implementation of the perforated plate control method inside microgas turbines with end user technical and economic benefits.

Towards achieving the main objective (O), the thesis is proposing to meet several specific objectives (SO) that might serve as milestones in the overall technological advancement:

- Numerical proof of concept on the ability of perforated plates accommodated to typical microgas turbine vaned diffuser to alter the shock structure (**SO1**)
- Experimental proof of concept on the ability of perforated plates to change the shock structure in cascade working environment (**SO2**)
- Design and manufacturing of a high-speed linear cascade typical for microgas turbines vaned diffusers configurations (**SO3**)
- Design and manufacturing of linearized microgas turbine diffuser vanes with perforated plate control regions included (**SO4**)
- Experimental validation on the ability of perforated plates to modify the shock structure and extend the operating range in a dedicated vaned diffuser linear cascade highly relevant for microgas turbines (**SO5**)

The workflow of the current thesis is presented in Figure 1-10. The activities are divided into three work packages (WP). The activities in WP1 are the starting point, evaluated at TRL 2, as they prove the feasibility and potential benefits of the perforated plate passive control strategy implemented inside vaned diffusers for miniaturized centrifugal compressors for microgas turbines (**SO1**). To increase the TRL to 4, two experimental work packages are run in parallel, with valuable feedback from WP2 to WP3 (marked with the purple arrow) regarding the perforated plate with cavity underneath geometrical parameters.

The main goal of WP2 is to transfer and validate the perforated plate passive control concept from single airfoil operation towards the cascade working environment (**SO2**). Side results of WP2 also include the study of perforated plate manufacturing techniques and the proper use of Schlieren optical diagnosis to investigate the change in shock structure dictated by the implementation of perforated plates with cavities underneath.

To achieve the main goal of WP3, and so the main objective of the current thesis, a high-speed vaned diffuser linear cascade is designed, manufactured and commissioned (**SO3**), closely replicating the vaned diffuser geometry developed in WP1. Both baseline vanes, with no control applied, and passively controlled vanes using the perforated plate with cavity underneath concept, are additively manufactured (**SO4**) with emphasis on the aerodynamic surface and control region quality. An extensive experimental campaign is performed at the end of WP3 to thoroughly document the contribution of perforated plates to reduce the shock induced losses and to increase the operating range of a vaned diffuser (**SO5**).

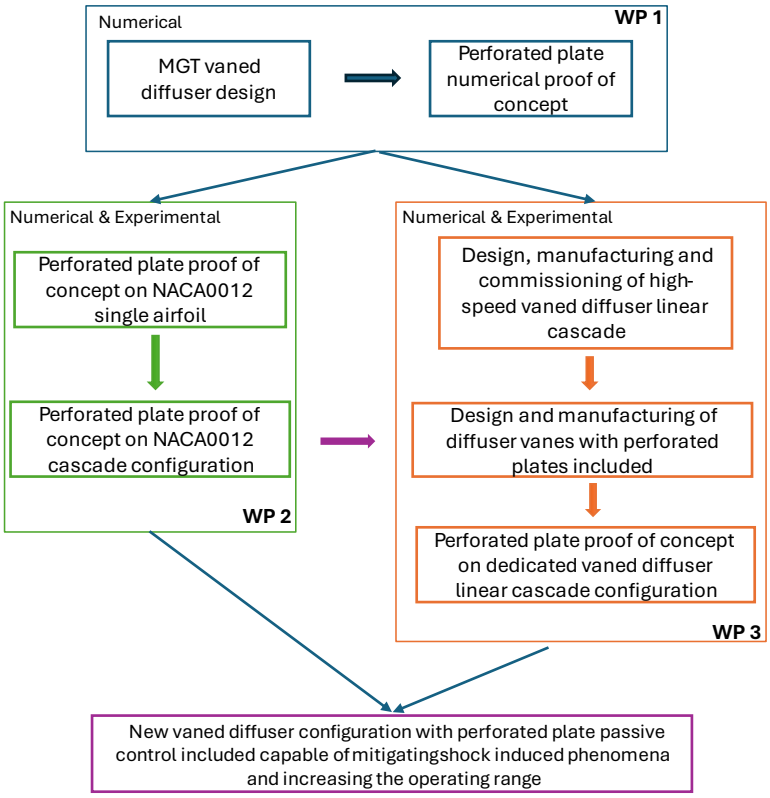

Figure 1-10 Workflow chart

1.4 Methodology

The methodology applied to achieve the above stated specific objectives involves analytical, numerical and experimental techniques, which are used either independent, or complementary, with results validation in between. Overall, the methodology applied in the current research includes:

- Literature review
  - with the help of Google Scholar or Web of Science search engines, a thorough review of scientific publications in the field of the PhD Thesis will be conducted. The review will target high impact factor publications from Web of Science, Scopus, IEEE or ScienceDirect database. Publication year filter will be applied to analyse the most recent publications first, and then, by cross-referencing, move to the pioneering studies in the field.
  - on one side, the literature synthesis will focus on microgas turbine engines and their centrifugal compressors to understand the design limitations and

possible paths to improve their efficiency or operating maps; on the other side, the literature review will address the perforated plate passive control method, with a focus on past applications figures of merit and manufacturing techniques, with the aim to find gaps and perspectives to accommodate them in cascade configurations typical for vaned diffusers
    - by leveraging the numerical and experimental approaches available from the literature, together with the author's findings, reservations and future work perspectives, the current thesis will address specific challenges towards the implementation of the perforated plate passive control method inside vaned diffusers for microgas turbine engines

- Experimental techniques
    - several manufacturing techniques for aerodynamic surfaces with perforated plates included will be investigated and the manufacturing methodologies shall be iteratively improved for a trade-off between cost, time and surface quality
    - high-speed wind tunnels and high-speed linear cascades shall be used as main testing environments together with high-speed Schlieren optical technique and pressure transducers
    - to reduce measurement errors, sensors calibration shall be performed in conjunction with numerical validation from CFD simulations
    - experimental uncertainties will be computed and reported to assure consistency and repeatability across the experimental campaigns

- Numerical modelling
    - advanced grid generation strategies for perforated plates together with modelling approaches will be developed in commercially available software using proper numerical schemes to capture high-speed associated phenomena
    - boundary conditions directly derived from experimental measurements shall be used to exactly replicate the testing environments and conditions

- Data processing
    - custom in-house scripts will be developed to handle experimental data and its statistical analysis (mainly T-student distribution for limited number of experimental samples)
    - numerical simulations data shall be processed with commercially available software, not only to validate the experimental results, but also to extend the analysis

For each specific objective, the tentative methodology is described below:

- **SO1** – The available scientific literature on diffuser databooks and statistical correlations will be used to design a baseline vaned diffuser. A literature review on the perforated plate passive flow control method shall provide the main geometrical parameters of the control region. The impact of perforated plates inside typical vaned diffusers will be numerically studied using shock capturing

numerical schemes. The most appropriate perforated plate numerical modelling will be investigated.

- **SO2 –** The optical access windows of a high-speed wind tunnel will be redesigned and manufactured to accommodate airfoils in cascade configuration. Several manufacturing techniques will be investigated for both baseline airfoils (no control applied) and passively controlled airfoils with perforated plates included. A Z-type Schlieren system including a high-speed camera will be used for flow visualization with a trade-off between frame rate, resolution and exposure time which maximise the quality. The static pressure on the bottom wall of the wind tunnel will be recorded via a scanivalve. For the final experimental campaign, the operating regime of the wind tunnel will be tuned such that, in the baseline configuration, strong normal shock waves are generated mid-chord inside the flow channels. All the other cascade configurations shall be tested at the same regime. Numerical simulations will be performed and compared against the experimental results.

- **SO3 –** Starting from the baseline annular vaned diffuser configuration designed part of SO1, a linearized version of the vaned diffuser will be generated and integrated into a dedicated high speed linear cascade test rig. Iterative design steps based on CFD results will be performed to achieve the desired flow features in the cascade. The entire facility shall be designed considering the experimental measurements to be carried out.

- **SO4 –** Several manufacturing techniques and methodologies using turbomachinery specific superalloys will be investigated for the production of linearized diffuser vanes with or without perforated plate passive control applied. High quality aerodynamic surfaces, rapid prototyping and reduced costs shall guide the final choice of the manufacturing process.

- **SO5 –** Commissioning tests will be conducted to check the entire facility is airtight and all the instrumentation delivers high-speed and reliable acquisition. In particular, the Schlieren images quality shall be verified if shock associated density gradients are visible and easy to be tracked. The final experimental campaign will be carried out at multiple flow regimes using baseline vanes and perforated plate passively controlled vanes. The experimental results will be compared and contrasted against the numerical ones.

CHAPTER 2 THESIS SUMMARY

The aim of the study in Chapter 2 is to design a vaned diffuser for an already existing centrifugal rotor, property of the National Research and Development Institute for Gas Turbines COMOTI. The application of the entire centrifugal stage is a 40 daN microjet engine, with primarily efficiency and size design requirements. The diffuser geometry developed in Chapter 2 serves as a baseline configuration used to investigate the implementation of perforated plates as passive flow control strategies inside diffuser cascade environments typical for microgas turbine engines.

The study presents a stepwise methodology for the entire diffuser design. The preliminary design is based on 0D/1D meanline codes and high R^2 statistical correlations, genuinely developed in Appendix C and D of the current thesis. All statistical correlations are generated from the microgas turbine engines and compressors' databases reported in Appendix A and B. The power law correlation in Figure 2-1 is used to estimate the 75 mm vaned diffuser shroud radius for a 40 daN input thrust. For the vaneless gap, stability design criteria are applied, to ensure that outlet flow angles and Mach numbers remain within stable operating ranges. For the vaned diffuser part, databooks and statistical correlations guided the design of vanes, considering factors like solidity, turning, diffusion factor and Reynolds number. Following the pre-design phase, 3D steady-state CFD simulations of the entire centrifugal stage are performed in Ansys CFX with structured grids generated using Ansys TurboGrid.

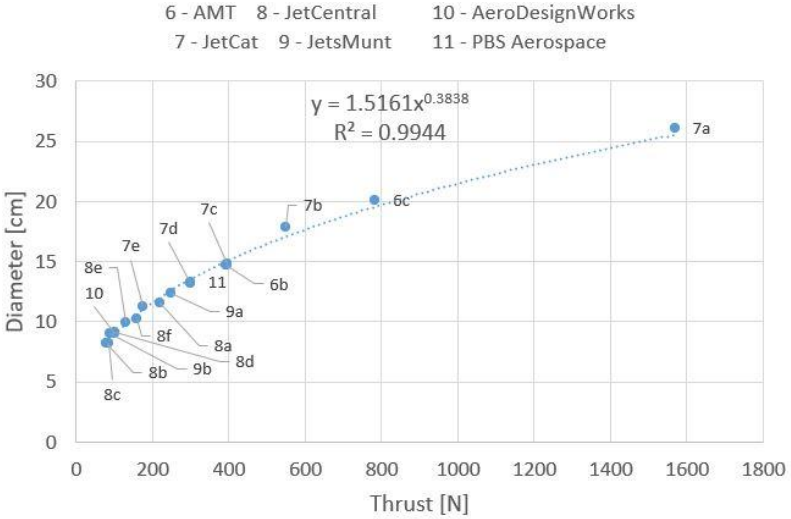

Figure 2-1 Diameter vs Thrust statistical design correlation
(source: Chapter 2 [27])

With design iterations and the use of high fidelity CFD modelling, the design methodology yields high total-to-total isentropic efficiency (84.1%), high total-to-total pressure ratio (4.78), a pressure recovery coefficient of 0.59 and an outlet flow angle of ~29° and can be considered as a guideline in the design of similar miniaturized vaned diffusers.

For the numerical proof of concept on the ability of perforated plates accommodated to typical microgas turbine vaned diffusers to alter the shock structure, three different diffusers are employed in Chapter 3, derived from the baseline vaned diffuser obtained in Chapter 2. The rotor used in Chapter 2, property of the National Research and Development Institute for Gas Turbines COMOTI, was frozen. The three diffusers' geometries in Chapter 3 include a low

solidity version and two high-solidity counterparts. The final diffuser candidate used for all subsequent experimental and numerical investigations in the current thesis, is depicted in Figure 2-2 and it includes 17 flow channels with main and splitter blades. The vaned diffuser channel height is 4 mm.

a. b. c.

Figure 2-2 Reference geometry of the MGT vaned diffuser with no control applied
a. full stage with rotor included b. annular vaned diffuser c. flow channel
(source: Chapter 6 [31])

For the numerical modelling of the perforated plate passive flow control technique inside vaned diffuser for microgas turbines in Chapter 3, the control cavity is generated in ICEM CFD as the direct extrusion of the structured grid elements from TurboGrid. The orifices of the perforated plate are then defined as permeable patches linking the fluid domain above and beneath the control cavity. According to the anchoring positions of the shock waves in the baseline, no control configuration, both the main and the splitter vanes accommodate two perforated plate control regions each, with 0.5 mm orifices and 0.5 mm cavity depth. The numerical simulations for the entire centrifugal stage are run for 68 000 rpm, with atmospheric inlet total pressure and outlet mass flow rate or static pressure, as boundary conditions. For 2.2 bara outlet static pressure, which corresponds to a high flow rate regime, a performance increase is recorded for the control case yielding 1% augmentation in isentropic efficiency and 0.03 bar reduction in overall total pressure loss. The performance increase is attributed to the ability of the perforated plates to reduce the shock waves intensities as shown by the density gradient contours at 50% channel height in Figure 2-3.

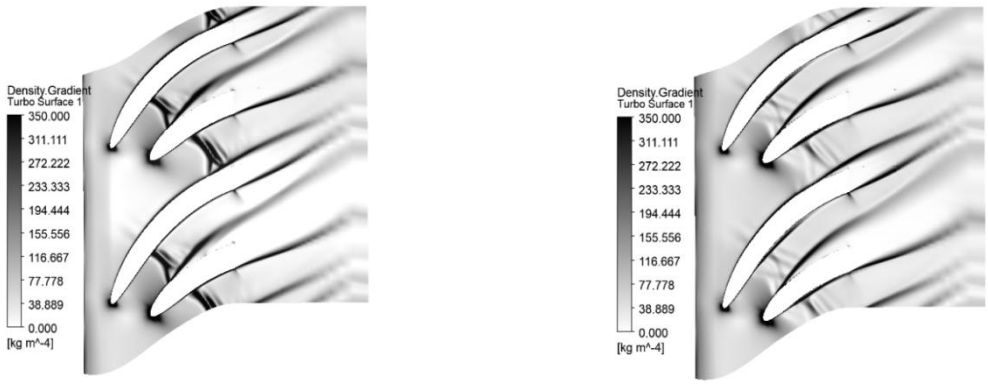

a. b.

Figure 2-3 Numerical density gradient – 50% channel height
a. no control b. passive control (source: Chapter 3 [28])

The study in Chapter 4 explores the use of perforated plates as a passive flow control method to improve the aerodynamic performance of NACA0012 airfoils and serves as a research methodology validation prior to studying perforated plate operation in cascade

environments, typical for microgas turbines vaned diffusers. The primary focus in Chapter 4 is on mitigating the detrimental effects of shock wave-boundary layer interactions (SBLIs), which occur in high-speed flows and lead to adverse pressure gradients, increased drag, and ultimately, efficiency loss. Additionally, the study investigates how perforated plates, placed on specific regions of a NACA0012 airfoil, alter the shock structure. By reducing the strength of shock waves and spreading the pressure gradient over a broader area, the study aims to evaluate improvements in total pressure loss and aerodynamic efficiency.

The experimental procedures employ a high-speed "Eiffel"-type open wind tunnel, capable of generating flows up to Mach 1.8. Key components of the experimental setup include a Z-type Schlieren system for visualizing shock waves structures, a static pressure measurement system using 18 pressure probes along the wind tunnel bottom wall and a batch of airfoils with perforated plates featuring orifice sizes ranging from 0.5 mm to 1.2 mm. The tests are conducted with airfoils mounted at a zero angle of attack. Each airfoil has one side unaltered (baseline) and the other equipped with a perforated plate and an underlying cavity for passive control. Complementing the experiments, steady-state 3D numerical simulations are conducted using Ansys FLUENT. The simulations use a density-based solver and the k-ω SST turbulence model. A 35 million elements unstructured mesh with localized refinements around the airfoil and perforated areas ensured accurate resolution of the flow, particularly related to the shock structures and boundary layer interactions. Boundary conditions for the simulations are derived from wind tunnel measurements, including inlet total pressure and outlet static pressure.

To ensure reliable experimental results, the study explores multiple manufacturing techniques for the NACA0012 airfoils with perforated plates:

- Multi-block PLA additive manufacturing: low-cost option that produces acceptable airfoil surfaces, but struggles with the assembling precision between the airfoil and the perforated plate.
- Inconel additive manufacturing: this method requires extensive post-processing due to surface roughness, leading to its temporary suspension.
- Single block PLA additive manufacturing: this technique provides high-quality results and it was chosen to produce the final experimental models with varying orifice size in the range 0.5-1.2 mm (Figure 2-4).
- Waterjet Cutting with Aluminum insert for the perforated plate (Figure 2-5): this method offers precise fabrication of small holes, but compromises the airfoil curvature in the assembling area between the airfoil and the perforated plate.

The airfoils fabricated using waterjet cutting and single block PLA additive manufacturing are ultimately selected for wind tunnel tests due to their superior surface quality and accuracy.

Figure 2-4 PLA 3D printed airfoils with multiple hole diameters (0.5 mm-1.2 mm) (source: Chapter 4 [29])

Figure 2-5 Waterjet cut airfoil and Aluminium insert for the control region (0.5 mm holes) (source: Chapter 4 [29])

Based on the high-speed Schlieren optical diagnosis, validated with the numerical simulations, the perforated plates effectively transformed strong, normal shock waves into λ-type shock structures as depicted in Figure 2-6. This change redistributes the pressure gradient, reducing the wave's intensity. As the orifice sizes of the perforated plates increases, the λ-type shock structures evolve into a series of weaker oblique compression waves. Overall, the introduction of perforated plates leads to slightly higher static pressures in the control region compared to the baseline case. This is attributed to the plates limiting local flow acceleration. The experimental static pressure data showed that as the orifice size increased, the minimum static pressure in the controlled region increased as well.

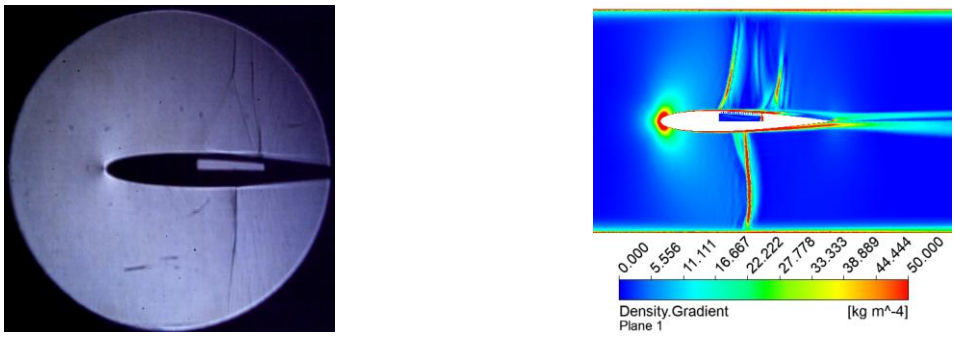

a. b.

Figure 2-6 Experimental vs numerical results
(upper surface – 0.5 mm perforated plate, lower surface – no control)
a. experimental Schlieren b. numerical Schlieren (source: Chapter 4 [29])

The numerical results for the baseline case with no control applied and the 0.5 mm case with perforated plate show that the control strategy provided a 0.2% reduction in total pressure loss compared to the baseline. This improvement is achieved through the favourable balance between reduced shock losses and increased viscous losses from the plate-induced roughness. Numerical simulations validated the experimental results, demonstrating close qualitative agreement in shock wave visualization (Figure 2-6) and pressure distribution (Figure 2-7).

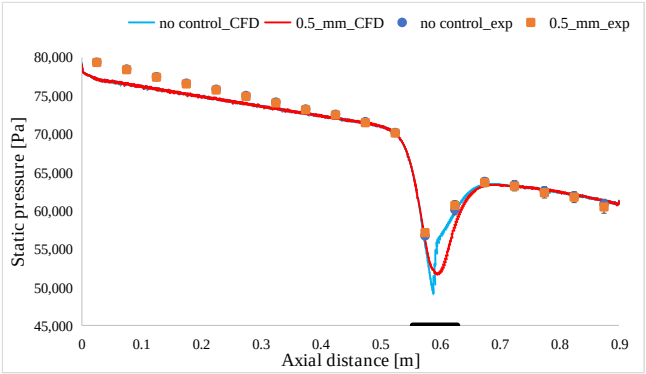

Figure 2-7 Static pressure distribution on the bottom wall of the wind tunnel
(source: Chapter 4 [29])

The study in Chapter 4 concludes that perforated plates might be an effective passive control strategy for improving aerodynamic performance in high-speed flows. The reduction in shock induced total pressure losses can outweigh the drawbacks of increased viscous drag due to perforated plate additional roughness. The research highlights the importance of optimizing orifice sizes and manufacturing techniques to maximize performance gains. Furthermore, the findings are the pillar for further studies in aeronautics and turbomachinery, especially in

cascade working environments, where managing shock wave-boundary layer interactions is critical for efficiency.

The study in Chapter 5 investigates the application of perforated plates with shallow cavities underneath as a passive control strategy to alter shock structures in a cascade configuration of NACA0012 airfoils, thus following the single airfoil proof of concept performed in Chapter 4. The main goal is to assess the effectiveness of the perforated plates in changing the shock waves structure in cascade working environment, highly relevant for high -speed turbomachinery applications.

Six different airfoil configurations, including a baseline setup without control and five configurations with varying perforation diameters in the range 0.5 mm-1.2 mm (Figure 2-8) are analysed. All airfoils' batches were additively manufactured using PLA. The perforated plates were mounted on both suction and pressure sides of the airfoils (Figure 2-9).

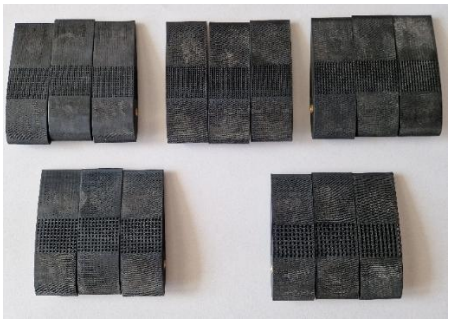

Figure 2-8 PLA 3D printed airfoils with multiple hole diameters
(0.5 mm, 0.65 mm, 0.8 mm, 1 mm, 1.2 mm)
(source: Chapter 5 [30])

Figure 2-9 Detail of PLA 3D printed airfoil with 0.5 mm hole diameter
(source: Chapter 5 [30])

The experiments are performed in the same "Eiffel"-type open wind tunnel used in Chapter 4, with capabilities for high-speed testing up to Mach 1.8. The setup includes Schlieren optical diagnostics for visualizing shock structures and static pressure taps along the tunnel bottom walls. The cascade setup consists of three airfoils aligned to achieve uniform null incidence. To accommodate the three-airfoil setup, the wind tunnel optical access windows were redesigned and manufactured.

To complement the experimental results for the baseline case and for the 0.5 mm perforated plate case, 3D steady-state RANS numerical simulations were run in Fluent using k-ω SST turbulence model. A 35 million cells unstructured computational grid was generated in Ansys Meshing using local refinements in the cascade region and in the perforated regions.

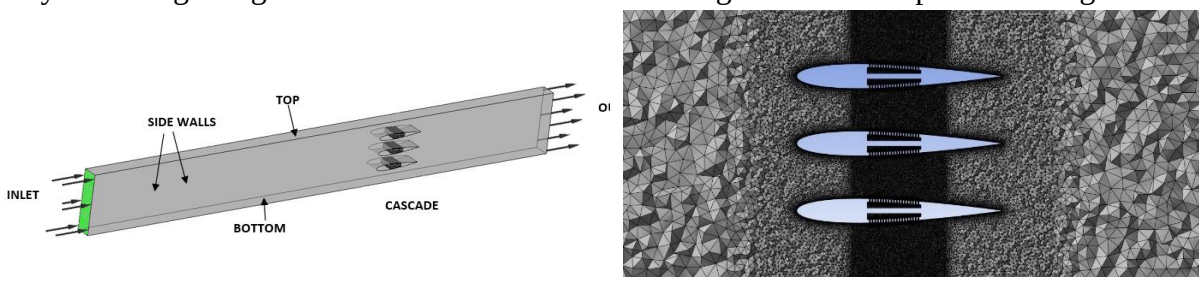

a. b.

Figure 2-10 Numerical simulation
a. computational domain b. grid detail for the passive control case (source: Chapter 5 [30])

In the baseline case, strong normal shock waves were observed, both numerically (Figure 2-13 a), and experimentally (Figure 2-11 a or Figure 2-13 c), by Schlieren. The introduction of perforated plates changed the normal shock configuration into a weaker "X-type" oblique shock pattern (Figure 2-13 b and Figure 2-11 b-f). Consequently, flow detachment downstream of the shock was reduced for airfoil 2, but some detachment persisted for airfoils 1 and 3 due to increased surface roughness. Numerically, improved static pressure recovery profiles were obtained (Figure 2-12) with gentle gradients in the controlled configurations which confirmed the reduced shock induced losses compared to the baseline case. The boundary layer thickened in the regions with perforated plates due to the recirculation and flow injections induced by the cavities. Despite shock intensity reduction was achieved, the mass-averaged CFD results showed an almost 2% increase in total pressure loss for the 0.5 mm control case compared to the baseline case with no control.

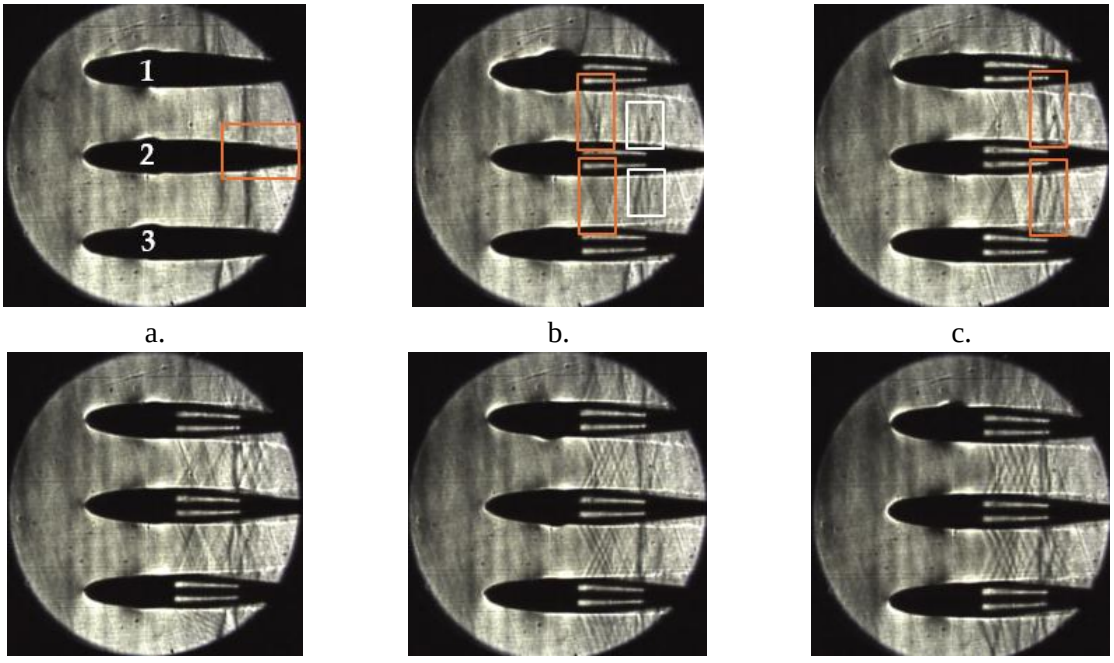

a. b. c.

d. e. f.

Figure 2-11 Schlieren images

a. baseline b. 0.5 mm c. 0.65 mm d. 0.8 mm e. 1 mm f. 1.2 mm (source: Chapter 5 [30])

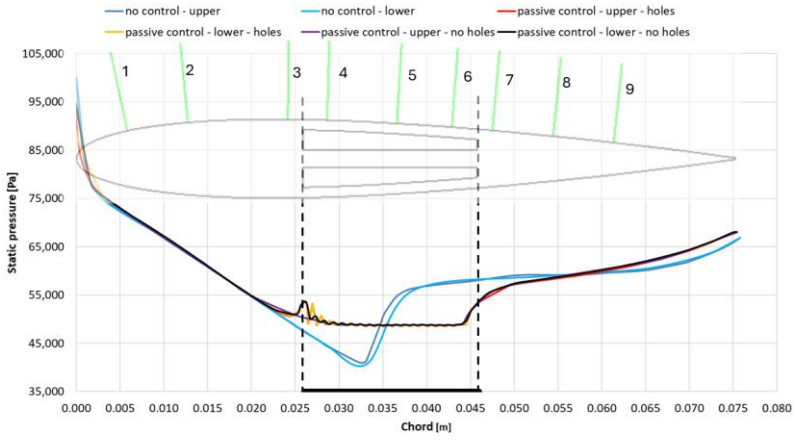

Figure 2-12 Static pressure distribution on airfoil 2 (baseline vs 0.5 mm control case) (source: Chapter 5 [30])

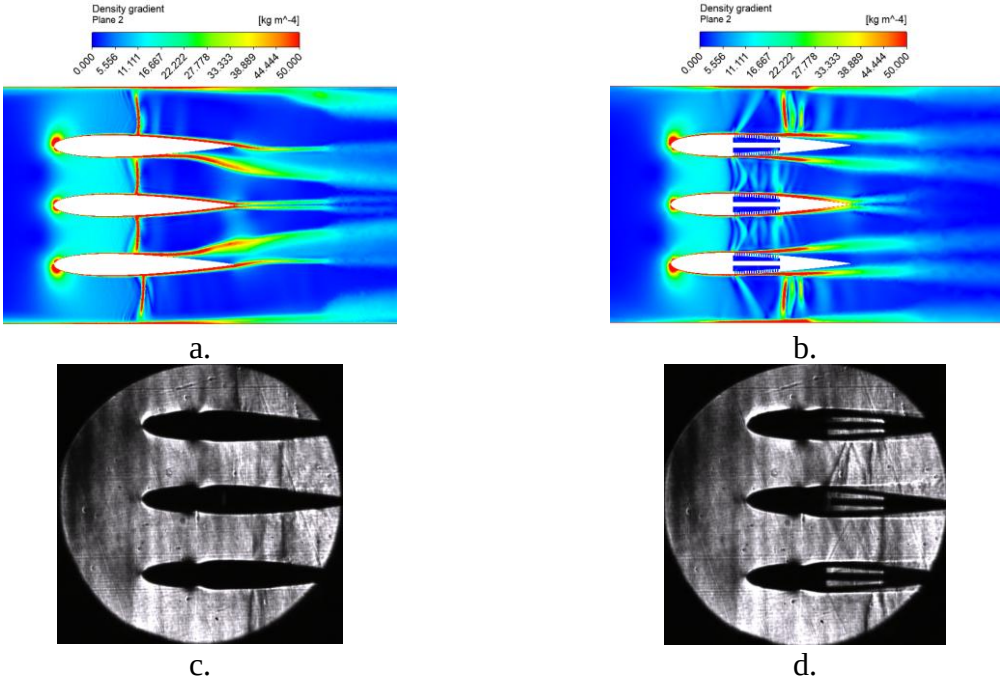

Figure 2-13 Qualitative comparison between CFD and experimental
a. no control CFD b. passive control 0.5 mm CFD
c. no control EXP d. passive control 0.5 mm EXP (source: Chapter 5 [30])

The study in Chapter 5 concludes that perforated plates are effective in changing the shock waves structure into weaker shock patterns in cascade environments indirectly reducing shock-induced losses. However, their effectiveness depends on the balance between reduced wave drag and increased viscous losses due to the intrinsic control mechanism of the perforated plate together with the additional roughness. The optimization of perforated plates geometric parameters, such as perforation size and distribution, can further enhance the performance.

The research in Chapter 6 presents the design and development of a high transonic linear cascade test rig aimed at studying shock wave structures in linearized centrifugal compressor vaned diffusers under various working conditions. High transonic shock wave structures are targeted inside the cascade as they represent a baseline configuration where the perforated plate passive control strategy can be applied, studied and validated in a more relevant turbomachinery working environment, as direct extension of studies presented in Chapter 5.

The design objective is to minimize experimental and computational resources by leveraging different flow regimes in the working channels thus exploring multiple operational points simultaneously, in a single experiment or simulation. For the preliminary definition of the linear cascade, the annular geometry of the baseline vaned diffuser designed in Chapter 2 (Figure 2-14 a) was intersected with a cylindrical surface at channel mid span and then unwrapped into a blade-to-blade representation (Figure 2-14 b). The vaned area was then extended into a complete linear cascade configuration (Figure 2-15) with proper inlet and outlet contoured walls to assure proper incidence and flow uniformity according to the original inlet conditions of the annular vaned diffuser.

RANS numerical simulations were conducted in Ansys CFX to simulate the flow behaviour and validate the presence of shock wave structures. Design iterations were performed with feedback from the CFD results to improve the flow characteristics in the linear cascade, minimizing inlet flow distortions and lateral wall effects. To further validate the numerical results, a grid convergence study monitoring the non-dimensional inlet-to-outlet total pressure

the was performed, with mesh resolutions ranging from coarse grids (7 million cells) to fine grids (36 million cells).

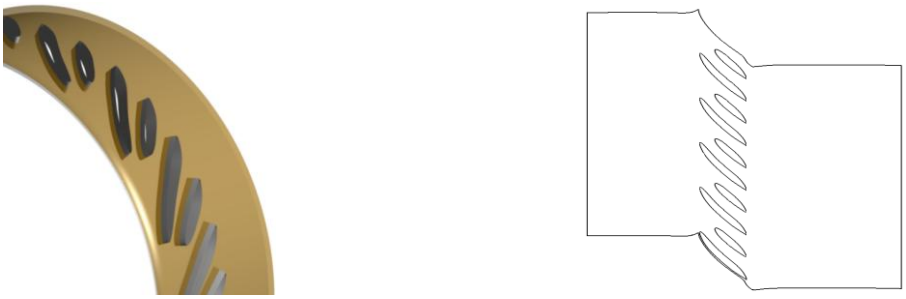

a. b.

Figure 2-14 Linearization procedure of the annular vaned diffuser configuration
a. cylindrical surface at 50% channel height b. unwrapped vaned diffuser (source: Chapter 6 [31])

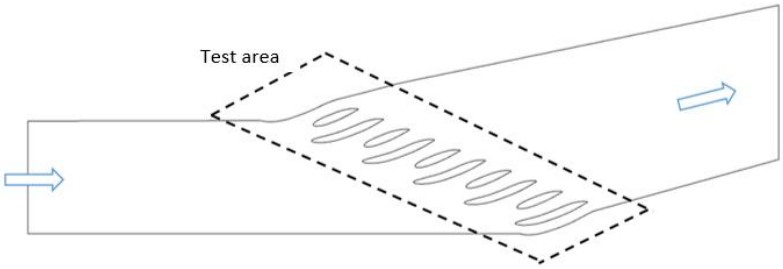

Figure 2-15 Linear cascade incorporating the linearized vaned diffuser
(source: Chapter 6 [31])

The final vaned diffuser linear cascade design in Chapter 6 shows a 9% difference in mass flow between the extreme flow channels of the cascade, slightly higher than the 5% difference in mass flow when the same channels are simulated individually with periodic boundary conditions. These slight variations in mass flow can be representative for different operating regimes at different isospeed lines of the vaned diffuser at off design points. The implementation of perforated plates in such configurations will assess the impact of the control strategy at multiple operating points emphasizing the way it alters the shock structure. The shock structures identified in this baseline design (Figure 2-16), prior to the application of flow control, range from normal strong shock waves inside main and secondary flow channels, to normal strong shock waves in the vicinity of the main blade leading edge where no confinement from a second wall is present. The latter operating environment is typical of single airfoil as a single vane wall defines the flow channel.

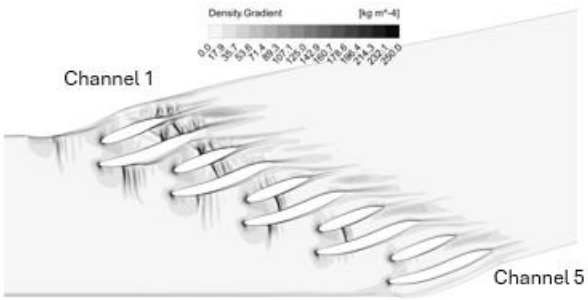

Figure 2-16 Density gradient contour in the cascade region – baseline (no control applied)
(source: Chapter 6 [31])

Localized acceleration zones near the leading edge and mid-chord regions of the splitter blades generate varying shock intensities across passages. The first two passages exhibit strong shock waves, but shock intensities diminish progressively from the first to the fifth passage. The pressure coefficient distribution on main and splitter vanes highlights the presence and intensity of shock waves.

The study in Chapter 6 successfully designed and validated a transonic linear cascade capable of exploring a wide range shock wave structures. The cascade replicates the operation of vaned diffusers for microgas turbine centrifugal compressors for various points on their operating map.

The vaned diffuser linear cascade designed in Chapter 6 was manufactured by milling, except the vanes, that were manufactured separately. The entire manufacturing methodology is described in Chapter 7. The main components that define the vaned diffuser linear cascade flow channel are depicted in the exploded view in Figure 2-16. Two plates are defining the flow channel: the back one, where the actual flow channel is milled and the front one that closes the flow channel and assures the correct channel clearances. Additionally, two covers are tightly screwed on the above-mentioned plates to assure proper alignment of the quartz optical access windows together with proper vanes clearances. An inlet adapter, additively manufactured by PLA, is also part of the test rig and it assures the smooth transition from the circular supply line coming from a high-pressure air tank to a rectangular inlet section in the linear cascade.

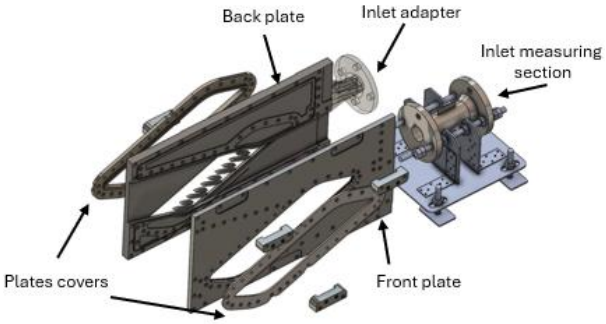

Figure 2-17 Linear cascade facility exploded view
(source: Chapter 7 [32])

The most challenging part of the test rig in terms of manufacturing was represented by the vanes, either in their baseline case, with no control applied, or in the passive control version, with several control regions applied. The control regions comprised checkerboard type perforated plates with 2 mm hollow cavities underneath. Several manufacturing iterations were performed before reaching a final solution that satisfied the desired surface quality of the vanes, on one side, and the quality of the perforated plates' orifices, on the other side. The turbomachinery specific superalloy Inconel 625 additive manufacturing technique by laser powder bed fusion (L-PBF) with selective laser melting (SLM) was the basis of all manufacturing iterations.

In the first iteration (Figure 2-18 a), several issues were identified related to the solid walls' thicknesses (especially at the trailing edge of the secondary blade model) which were too thin to be built by the laser. Additionally, the nominal 0.5 mm orifice size, together with the spacing in between the holes, were too stringent for the manufacturing capabilities and precision. The deviation of the holes from the circular shape was too high and some of the orifices were not completely pierced, leading to a poor overall quality of the perforated plate which might have affected the proper passive control operation during the experiments. Therefore, the orifice size

was modified to 0.75 mm due to technological reasons, and the distance in between the holes was changed accordingly to 2.6 times the new nominal diameter of 0.75 mm chordwise and to 1.5 times spanwise. For final roughness control, the sandblasting technique was applied. However, the final quality of the flow surface was not satisfactory and further milling processes were proposed for future design iterations. This implied material additions to all models' dimensions for surface quality control by machining and the integration of a platform to the model's bases to facility CNC clamping (Figure 2-18 b). To further refine the manufacturing process in the second iteration (Figure 2-18 c), the ends of the experimental model base platform were rounded to diminish the material losses and to protect the SLM machine scraper.

The final manufacturing procedure consisted in turbomachinery specific superalloy Inconel 625 additive manufacturing by laser powder bed fusion (L-PBF) with selective laser melting (SLM), followed by electroerosion and CNC milling for roughness control (Figure 2-19). The combination of these three manufacturing procedures was specifically chosen to compensate for the limitation each method intrinsically possesses. The individual vane was manufactured as single block to allow a smooth transition between the vane surface and the control region. Judging the small size and the distribution of the orifices in the control region, traditional drilling methods were abandoned. The vanes underwent thorough dimensional control in the form of surface roughness analysis and a maximum deviation of ±0.04 mm from the CAD model was recorded, thus confirming the precise manufacturing process. Apart from the high surface quality achieved by the manufacturing approach, the study in Chapter 7 is also very relevant to aeronautical industry, where nickel-based superalloys are commonly used in turbomachinery blades. The final configuration of the passively controlled vanes is characterized by the following geometrical features:

- the main vane incorporates two perforated plate control regions. The first one is located close to the suction side leading edge, and it has 12 mm length with 8x7 orifices in checkerboard arrangement. The second control region is located mid-chord on the pressure side, and it has a length of 27 mm with 13x8 orifices. For both control regions, the cavity depth is 2 mm.
- the secondary vane includes two identical perforated plate control regions, both located mid-chord. The length of the control region is 22 mm with 11x8 orifices arranged in checkerboard pattern. The depth of the control cavity is 2 mm.

a. b. c.

Figure 2-18 Linearized diffuser vanes during the manufacturing process
a. 1st iteration b. 2nd iteration c. 3rd iteration (source: Chapter 7 [32])

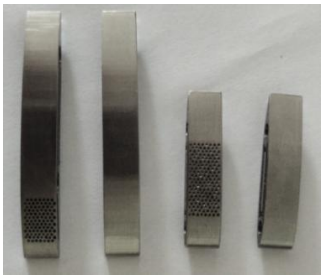

a.

b.

c.

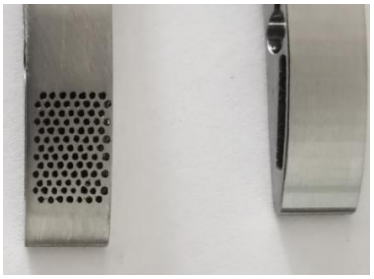

d.

Figure 2-19 Vanes after milling for surface finishing (no control and passive control)
a. top view b. side view c. main vane with passive control during the manufacturing process d. main blade leading edge detail –no control and passive control (source: Chapter 7 [32])

Besides the vanes' manufacturing that was critical in the test rig development in Chapter 7, their alignment and sealing within the lateral walls in the cascade was also of utmost importance to ensure proper incidence conditions for the entire cascade. The alignment was achieved by a control pattern milled in the quartz optical access windows that closely replicated the vane contour (Figure 2-20). The sealing with the quartz windows was done with two Teflon screws (Figure 2-21) which also possess vibration absorption capabilities.

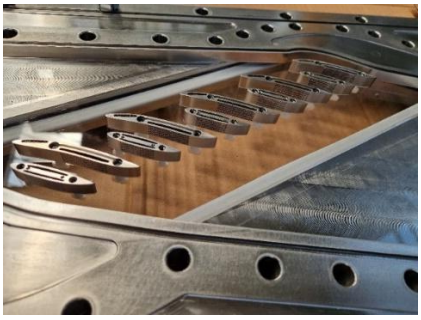

Figure 2-20 Vanes with passive control -front plate quartz optical access window (source: Chapter 7 [32])

Figure 2-21 Vanes with their mounting screws (source: Chapter 7 [32])

Before commissioning tests, the air supply line was instrumented with a static pressure and a total pressure sensor (in the region of the inlet adapter) and a flowmeter to allow the precise definition of future boundary conditions for the numerical simulations used for validation. The piping and instrumentation diagram of the test rig is depicted in Figure 2-22. To exploit the optical access (Figure 2-23), a Z-type Schlieren system was aligned to capture the flow features evolution in the vanes region focusing on shock structures density gradients (Figure 2-24). Before commissioning test, test readiness review was performed (Figure 2-25).

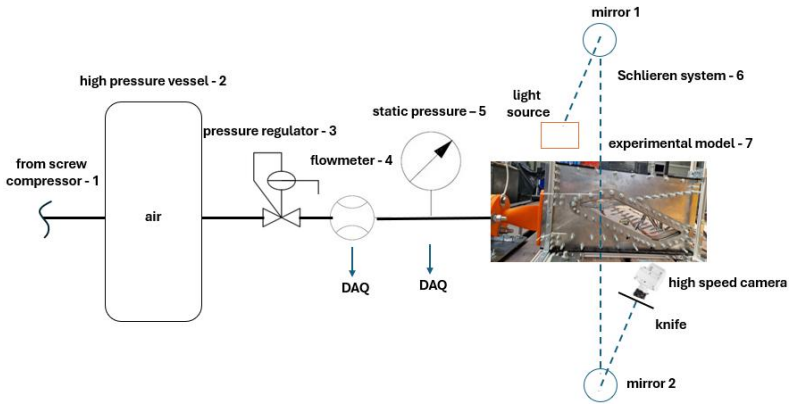

Figure 2-22 PID diagram for linear cascade facility
(source: Chapter 7 [32])

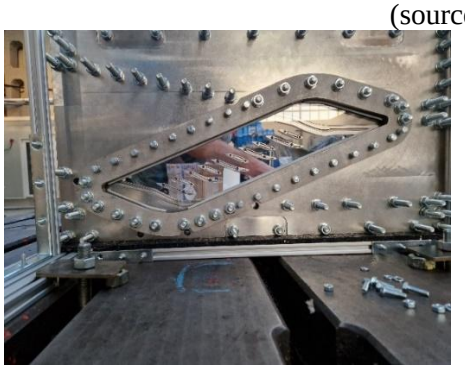

Figure 2-23 Linear cascade side view exploiting optical access
(source: Chapter 7 [32])

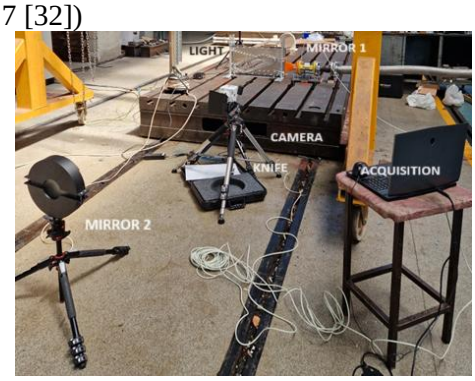

Figure 2-24 Schlieren system for flow visualization
(source: Chapter 7 [32])

Figure 2-25 Facility overview – after test readiness
(source: Chapter 7 [32])

Several commissioning tests were conducted in Chapter 7, solely using the baseline vanes with no control applied, to check that the entire facility, including instrumentation, was working properly according to the design specifications. Different inlet gauge static pressures ranging from 0.7 bar to 0.9 bar were set, resulting in multiple shock characteristics, which stronger shocks at elevated tested pressures. The shock structures were located in the main and secondary channels, and also in proximity to the main blades' leading edges. No malfunction in the air supply system or data acquisition was recorded.

The commissioned vaned diffuser linear cascade from Chapter 7 was involved in the final experimental campaign of the current thesis disseminated in Chapter 8. Both the baseline geometry with no control applied on the vanes and the geometry with perforated plates accommodated on the vanes were experimentally investigated at several inlet gauge static pressures ranging from 0.7 bar to 0.9 bar (Figure 2-26-Figure 2-29). Apart from the inlet static

pressure and the mass flow rate data during testing, the focus was on the analysis of the Schlieren images with the final goal to assess the perforated plate influence on the shock structure and on the boundary layer.

For all tested regimes in Chapter 8, the normal shock waves that appear in the baseline operation of the cascade were converted by the control strategy into either less intense oblique compression structures anchored to the control region, or even weaker aeroacoustic wave trains with a given angle relative to the cascade (see rectangular highlights in Figure 2-26-Figure 2-29). A different behavior was observed for the main blade leading edge at 0.9 inlet gauge static pressure. The initial normal shock wave in the baseline case was converted into a λ-type shock structure typical for single airfoil operation. This is justified by the lack of a second wall in the leading-edge area to fully confine the flow which is similar to isolated airfoil flow conditions. Despite the perforated plates successfully attenuated the shock intensity, specific issues arose related to the flow detachment areas as a direct result of the blowing effect from the cavity underneath, combined with the enhanced roughness of the perforated area. Boundary layer detachment is emphasized by the Schlieren system in proximity of the main blade leading edge and in the splitter blades control areas.

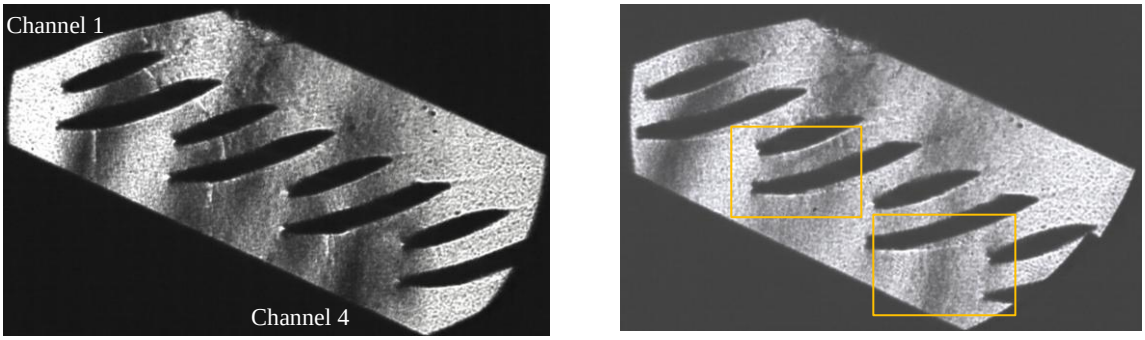

a. b.

Figure 2-26 Schlieren snapshots – 0.7 bar gauge inlet static pressure
a. no control b. passive control 0.75 mm (source: Chapter 8 [33])

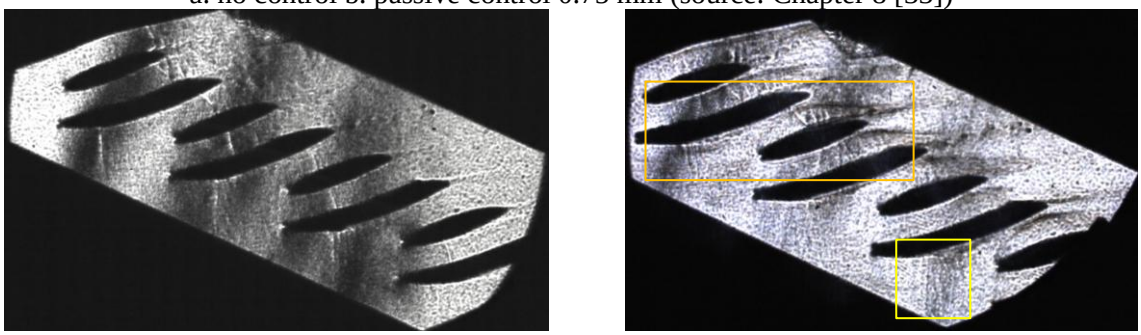

a. b.

Figure 2-27 Schlieren snapshots – 0.8 bar gauge inlet static pressure
a. no control b. passive control 0.75 mm (source: Chapter 8 [33])

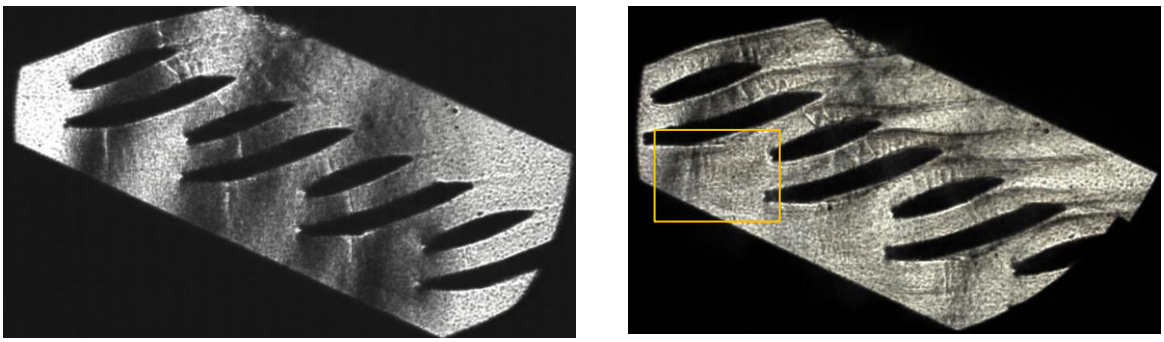

a. b.

Figure 2-28 Schlieren snapshots – 0.85 bar gauge inlet static pressure
a. no control b. passive control 0.75 mm (source: Chapter 8 [33])

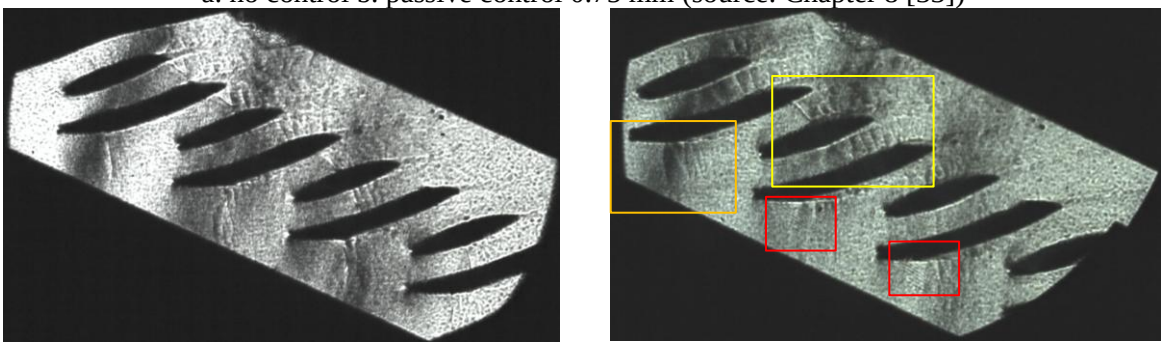

a. b.

Figure 2-29 Schlieren snapshots – 0.9 bar gauge inlet static pressure
a. no control b. passive control 0.75 mm (source: Chapter 8 [33])

The experimental results for the 0.8 bar gauge inlet pressure with passive control applied showed a 4% mass flow rate augmentation compared to the baseline case, with nearly identical inlet conditions from the air supply line, as shown in Figure 2-30.

The 0.8 bar experimental results were also numerically validated by CFD simulations for both the baseline and the passive control cases. The numerical boundary conditions were imposed using the experimental inlet total pressure and outlet static pressure (Figure 2-31 a). The computational domain was discretized using Ansys Meshing into a 65 million cells unstructured grid with local refinements in the cascade region, perforated plates control area and lateral walls of the entire domain (Figure 2-31 b and c).

The numerical Schlieren plots in terms of density gradient (Figure 2-32) followed the experimental results as they also emphasized a change in shock structure from single normal shock to tiny compression trains with a fixed anchoring angle with respect to the blade surface. The numerical results also depicted the direct influence of the perforated plate in flow separations corresponding to the control region. This directly impacted on the overall total pressure loss, that was not significantly different from the one computed in the baseline configuration. Thus, the reduction in shock induced total pressure loss was exceeded by augmented viscous losses as a direct consequence of the perforated plate accommodation on the vanes' aerodynamic surfaces.

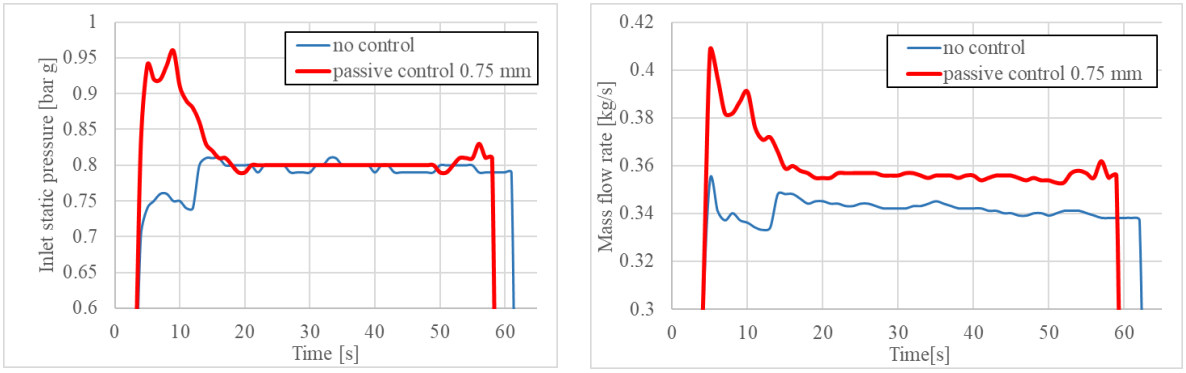

a. b.

Figure 2-30 Experimental rig parameters for 0.8 bar gauge test
a. inlet static pressure b. mass flow rate (source: Chapter 8 [33])

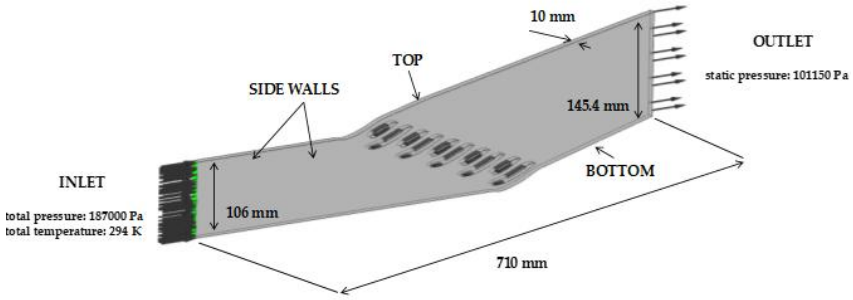

a.

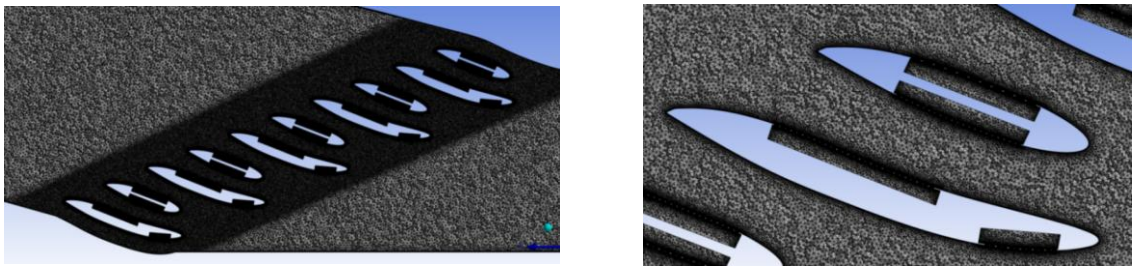

b. c.

Figure 2-31 Computational domain
a. overview b. grid c. grid detail (perforated plates) (source: Chapter 8 [33])

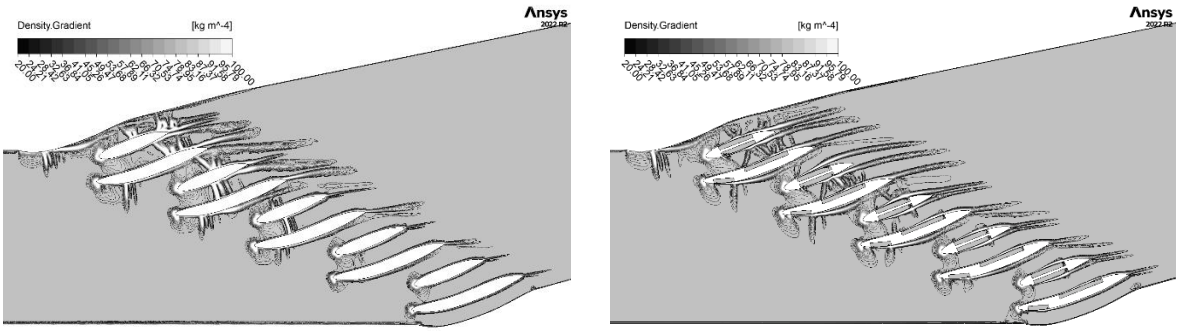

a. b.

Figure 2-32 Density gradient distribution – mid plane
a. no control b. passive control (source: Chapter 8 [33])

Compared to the shock structure alteration with the in-line orifice array pattern in Chapter 4 and 5, the checkerboard type perforated plate in Chapter 8, converted the initial strong normal shocks into highly regular wave formations, aeroacoustic in nature, with low intensity, whose wave front inclination almost coincides with the cascade complementary angle (Figure 2-33 and

Figure 2-34). As the hole pattern follows a staggered, checkerboard-type arrangement, with alternating row of orifices, the lack of a continuous surface between adjacent rows of perforations, similar to the one present in the in-line orifice pattern, may have enhanced the visibility of the phenomenon.

The shape and regularity of the aforementioned wave trains in vicinity of the perforated plate control region showed a different behaviour in comparison with the single airfoil results in Chapter 4. For the in-line orifice distribution in Chapter 4, the emerging point of the oblique shock waves is on the airfoil, in between two rows of holes. Moreover, their angle is given by the leading oblique shock wave that form instead of the initial normal shock wave (when no control is applied). The endpoint of all the small oblique shock waves is on the second limb of the λ-type shock structure. With the checkerboard type hole arrangement, the waves emanate at a certain angle from the surface, but they are not attached to the surface itself. Additionally, there is no sharp endpoint of the waves, they lose intensity as they move away from the perforated surface, acting as a pattern of open ended tubular acoustic resonators.

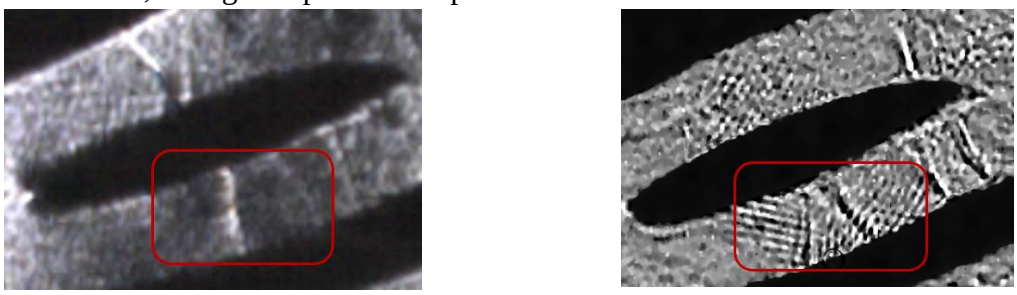

a. b.

Figure 2-33 Detailed view of shock structure – first splitter
a. no control b. passive control (source: Chapter 8 [33])

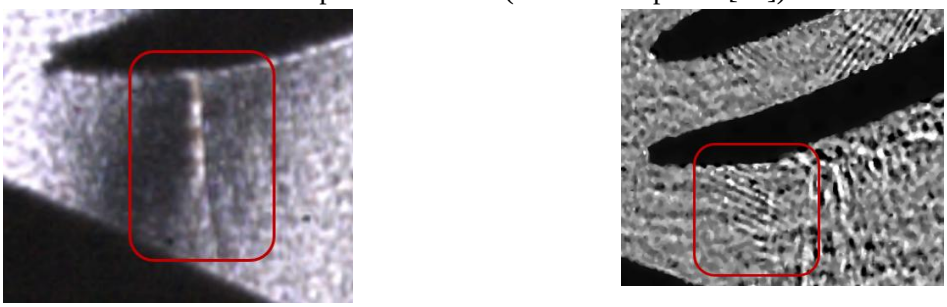

a. b.

Figure 2-34 Detailed view of shock structure – second main blade
a. no control b. passive control (source: Chapter 8 [33])

Eventually, the experimental data revealing the intrinsic change of the normal shock structures into highly regular wave formations with precise angle with respect to the blade surface was supported by simplified aero-acoustic analytical modelling, by ultimately approximating the cavity underneath the perforated plate as a Helmholtz resonator. The model yielded a 1.048 mm wavelength, very close to the one estimated from the optical Schlieren diagnosis of 1.1 mm. Moreover, a thorough optical analysis of the tiny shocks train angle relative to the blade surface showed a value very close to the complement of the cascade stagger angle.

CHAPTER 3 CONCLUSIONS

3.1 General conclusions and thesis novelty

The passive control method involving a perforated plate with hollow cavity underneath is genuinely applied in the current thesis in vaned diffusers cascade arrangements, typical for microgas turbines. According to the available scientific literature, the perforated plate passive control technique was extensively investigated for shock boundary layer interaction control for single airfoils and helicopter blades in external aerodynamics or for internal walls of nozzles and supersonic intakes. All the available research background related to perforated plates was thus the starting point of the current thesis.

The present work extends the research efforts dedicated to perforated plate control strategy by applying it to a new working environment, namely the cascade arrangement, where typical flow effects arise due to additional confinement by the vanes' walls. Starting from single airfoil validation, a roadmap is followed towards a final proof of the concept on the use of perforated plates inside typical vaned diffusers for microgas turbines. Hence, the novel character of this work stems directly from the application of an already existing flow control technique into a new operating environment where particular high-speed fluid dynamics phenomena appear. Additionally, the novelty is also supported by the fundamental NACA 0012 linear cascade studies on the perforated plates orifice size which are pioneering the parametric studies for this type of passive flow control technique applied to cascade configurations.

The current thesis increased the TRL from 2 to 4 (see Figure 3-1) through experimental testing of a technological demonstrator that integrates a linearized vaned diffuser with a perforated plate passive flow control system. TRL 2 was supported by CFD studies which could explore the potential benefits and feasibility of using perforated plates in vaned diffusers. To the author's knowledge, when the work started, there were no physical prototypes in the turbomachinery field to study this aspect. To advance the maturity level, preliminary experimental studies with either single airfoils or cascade configurations were performed inside a high-speed wind tunnel to thoroughly assess the effect of perforated plates of varying orifices on the shock structure and on the overall losses budget.

A high-speed linear cascade mapping the initially designed vaned diffuser was developed, manufactured and commissioned part of the current thesis. The linear cascade was designed to allow the visualization of the high-speed fluid flow with its associated SWBLI phenomena using high-speed Schlieren techniques. The metal additive manufacturing of vane prototypes with perforated control regions aimed high quality surfaces and control regions (orifices and cavities), supporting the development of a complete methodology for fabricating components with perforated control regions featuring hollow cavities underneath.

Data measured during the final experimental campaign, along with comparisons to numerical results, constitute another factor supporting the feasibility and performance of the perforated plate technology employed in vaned diffusers. The use of perforated control regions led to a reduction in the intensity of shock waves and a 4% increase in flow rate through the passively controlled system compared to the baseline classical case. This suggests the readiness for more extensive testing and potential application in relevant environments for even higher TRL. Additionally, the results demonstrate that the technology is validated under controlled

laboratory conditions and can be considered a good candidate for further development and scaling.

3.2 Personal contributions

With a roadmap to achieve the stated objectives for the current thesis, the entire workload was divided into well-defined activities with measurable results that eventually lead to a series of personal contributions to the microgas turbines scientific community. As emphasized in the following description, the personal contributions (**PC**) are tightly linked to the specific objectives (**SO**).

On one side, the personal contributions are related to the perforated plate passive control strategy proof of concept when applied to cascade configurations and particularly to vaned diffusers for microgas turbines centrifugal compressors:

- **Implementation of advanced structured grid generation strategies for perforated plates numerical modelling (PC1)**. The structured grid generation for the perforated plate control region brought some intrinsic meshing difficulties in Chapter 3. The cavity fluid cells were generated as direct element extrusion from the aerodynamic surface. The perforated plate' orifices were subsequently defined numerically as permeable, fluid to fluid interfaces. The simulations in Chapter 3 numerically proved the change in shock structure when perforated plates with cavities underneath are applied to vaned diffusers for microgas turbines (**SO1**).

- **Proof-of-concept for perforated plate passive control technique on NACA0012 single airfoils with different orifice sizes (PC2).** The study in Chapter 4 served as an initial validation of the proper experimental and numerical techniques used to investigate the impact of perforated plates on the shock structure alteration in single airfoil high-speed flows. The perforated plates showed a direct impact on the shock structure: a strong unique normal shock was converted into a λ-type shock structure, for small orifices, or a weak oblique compression train, for large orifices. The studies of varying orifice perforated plates applied to single airfoils, including the manufacturing methodology, were the pillar for the implementation of the perforated plate passive flow control technique to cascade environments with the final goal to achieve **SO2**.

- **Proof-of-concept for perforated plate passive control technique on NACA0012 cascade configurations with different orifice sizes (PC3).** An intermediate perforated plate proof of concept study between the single airfoil in Chapter 4 and the vaned diffuser cascade in Chapter 8 was the NACA 0012 cascade configuration in Chapter 5. Perforated plates with varying orifices in the range 0.5-1.2 mm were genuinely applied on both the upper and lower surface of three NACA 0012 airfoils arranged in cascade configurations. The numerical results, together with the Schlieren images, showed a transition from strong normal shocks to weaker oblique 'X-type' compression pattern whose interaction complexity depends on the orifice size (**SO2**).

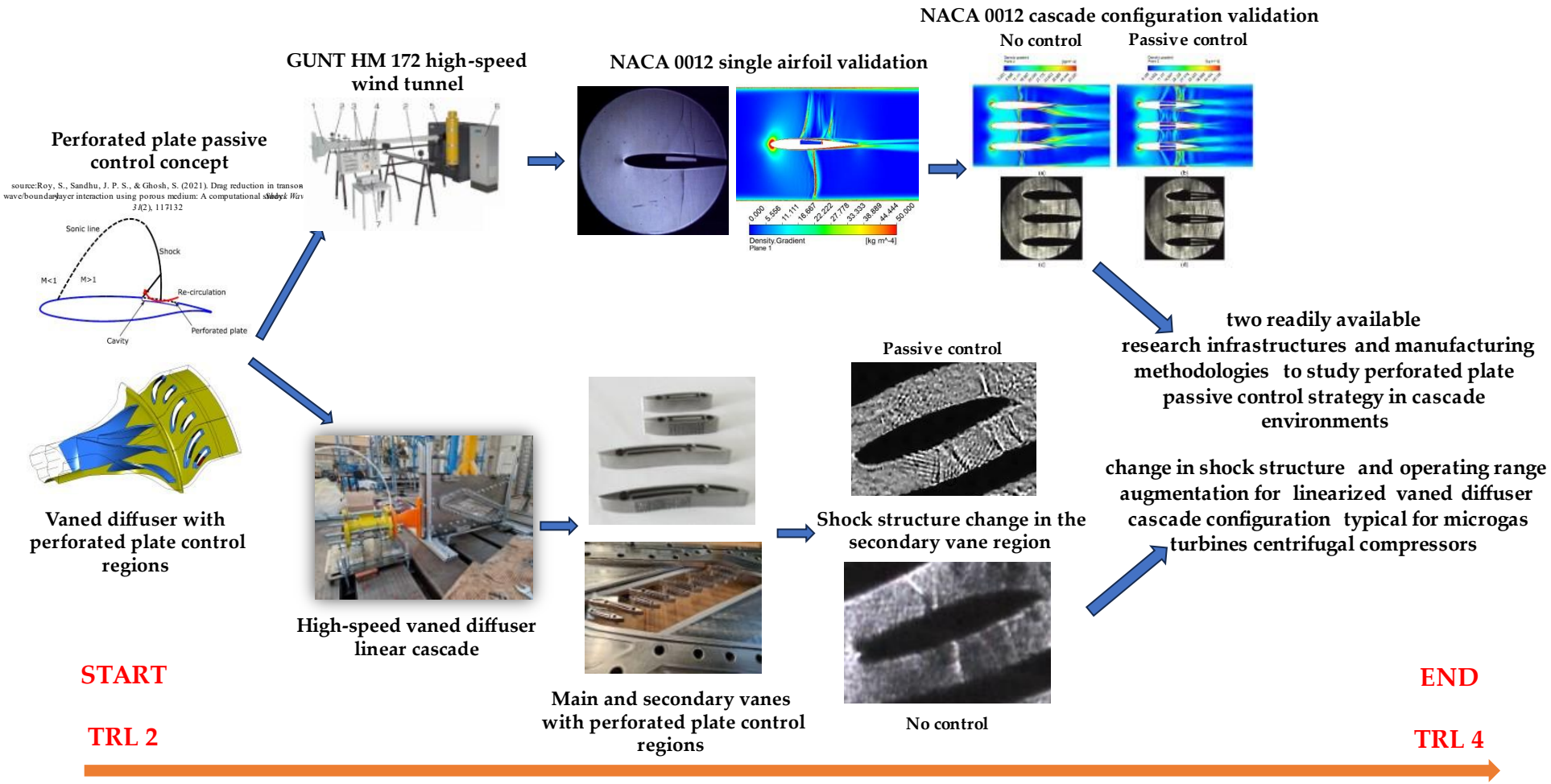

Figure 3-1 TRL advancement roadmap

- **Perforated plate passive control technique validation on dedicated vaned diffuser linear cascade configuration (PC4).** The perforated plate passive control technique applied to typical diffuser vanes was experimentally and numerically investigated in Chapter 8. The results confirmed the operating principle of the control method and revealed a change in shock structure from strong normal to either less intense oblique compression structures anchored to the control region, or even weaker aeroacoustic wave trains with a given angle relative to the vane surface which coincides with the cascade complementary angle. The experimental results showed a 4% mass flow rate augmentation in the passively controlled case compared to the baseline reference case with no control applied (**SO5**). Based on the results regarding perforated plate orifice size parametric study on the NACA 0012 cascade in Chapter 5, the final linearized diffuser vanes configurations that achieved positive passive control effects resulted as a trade-off between manufacturing capabilities, cost and gas dynamics phenomena. Compared to the in-line orifice array pattern used in Chapter 4 and Chapter 5, the checkerboard type perforated plate with hollow cavity underneath, employed in Chapter 8, redistributed high-intensity shock waves into highly regular wave formations with low intensity which emphasized different patterns than those for single airfoils. This was attributed to control cavity aeroacoustic phenomena which was further supported by an analytical modelling validated against the available experimental data.

- **Development of pre-design correlations based on microgas turbines databases and miniaturized centrifugal compressors' databases (PC5).** Based on the available performance data for microgas turbines and miniaturized centrifugal compressors, accurate correlations with high R^2 values were generated in Appendix C and D and used in Chapter 2. All statistically established correlations will ease the pre-design phases where some initial guesses are mainly based on the existing literature.

On the other side, the personal contributions are related to experimental activities, namely development of research infrastructures and methodologies to investigate the perforated plate passive control strategy in cascade configurations and, more specific, to vaned diffusers for microgas turbines:

- **Analysis of manufacturing techniques dedicated to symmetrical airfoils with perforated plate passive flow control technique applied on their aerodynamic surfaces (PC6)**. The study in Chapter 4 involved either multi-part manufacturing (water jet cut airfoil with laser drilled aluminum perforated plate attached or PLA additively manufactured airfoil with PLA additively manufactured perforated plate) or single-block approaches (Inconel 625 selective laser melting (SLM) additive manufacturing or PLA additive manufacturing). The final single-block PLA additive manufactured airfoils showed acceptable accuracy of the perforated plate orifices in the range 0.5 mm – 1.2 mm. The results in Chapter 4 highly supported the achievement of **SO2**.

- **Reconfigurations of a high-speed wind tunnel to accommodate a NACA 0012 linear cascade (PC7).** The GUNT HM172, as delivered by the manufacturer, solely allows single object testing, either aerodynamic or bluff body. The activity in Chapter

5 involved the manufacturing of new optical access windows and anchoring mechanisms, while assuring airtight capabilities of the entire facility. The latter was of utmost importance to minimize the experimental error in the bottom wall static pressure measurement and in the overall operation of the perforated plate which involves a flow recirculation in a cavity underneath. The high-speed wind tunnel reconfiguration to accommodate cascade configurations was the pillar to achieve **SO2**.

- **Commissioning of a versatile high-speed linear cascade dedicated to centrifugal compressors' vaned diffusers suitable for microgas turbines (PC8)**. The facility designed in Chapter 6 and commissioned in Chapter 7 (**SO3**), can accommodate a wide range of vanes geometries, from baseline ones, with no control applied, to passively controlled ones using perforated plates. By rapid prototyping of vanes according to the manufacturing techniques presented in Chapter 7, extensive experimental studies can be performed. Additionally, the design versatility of the entire test rig allows for subsequent improvement in the experimental techniques applied, ranging from optical diagnosis to high-speed wall static pressure measurements.

- **Analysis of manufacturing techniques dedicated to linearized diffuser vanes with perforated plate passive flow control technique applied on their aerodynamics surfaces (PC9)**. The study in Chapter 7 involved turbomachinery specific superalloy (Inconel 625) selective laser melting (SLM) technology combined with several post-processing techniques ranging from sandblasting to electroerosion and high-precision milling. The final manufacturing chain for the linearized microgas turbine diffuser vanes (**SO4**) involved Inconel625 SLM followed by electroerosion and high precision milling. The achieved accuracy compared to the ideal CAD model was within 0.04 mm. The entire design and manufacturing methodology developed in the current work serves as a pillar for future parametric studies on the perforated plates geometrical features, allowing rapid, high-quality and cost-effective vanes prototyping.

PUBLICATIONS AND PROJECTS

I. Publications in WOS journals in the field of PhD thesis

- **Gall, M.**, Dumitrescu, O., Drăgan, V., & Crunțeanu, D. E. (2024). Effects of Perforated Plates on Shock Structure Alteration for NACA0012 Airfoils. *Inventions*, *9*(2), 28, https://doi.org/10.3390/inventions9020028; WOS:001210107500001; ISSN: 2411-5134

- **Gall, M.**, Dumitrescu, O., Drăgan, V., & Crunțeanu, D. E. (2024). Effects of Perforated Plates on Shock Structure Alteration for NACA0012 Cascade Configurations. *Inventions*, *9*(5), 110, https://doi.org/10.3390/inventions9050110; WOS:001340920700001; ISSN: 2411-5134

- **Gall, M.**, Drăgan, V., Dumitrescu, O., Prisăcariu, E. G., Condruz, M. R., Paraschiv, A., Petrescu, V., & Vlăduț, M. (2024). Design, Fabrication, and Commissioning of Transonic Linear Cascade for Micro-Shock Wave Analysis. *Journal of Manufacturing and Materials Processing*, *8*(5), 201, https://doi.org/10.3390/jmmp8050201; WOS:001340893800001; ISSN: 2504-4494

- Dumitrescu, O., **Gall, M.**, & Drăgan, V. (2023). A Three-Dimensional Design to Study the Shock Waves of Linear Cascade with Reduced Mass Flow Requirements. *Applied Sciences*, *13*(19), 11029, https://doi.org/10.3390/app131911029; WOS:001114360800001; ISSN: 2076-3417

- Drăgan, V., Dumitrescu, O., **Gall, M.**, Prisăcariu, E. G., & Gherman, B. (2024). Experimental Identification of a New Secondary Wave Pattern in Transonic Cascades with Porous Walls. *Aerospace*, *11*(11), 946, https://doi.org/10.3390/aerospace11110946; WOS:001363587000001; ISSN: 2226-4310

II. Publications in WOS journals in complementary fields of the PhD thesis

- Cican, G., **Gall, M.**, Bogoi, A., Deaconu, M., Crunțeanu, D.E. (2023) Experimental Investigation of a Micro Turbojet Engine Chevrons Nozzle by Means of the Schlieren Technique. *Inventions*, *8*, 145, https://doi.org/10.3390/inventions8060145; WOS:001130908000001; ISSN: 2411-5134

- Bogoi, A., Cican, G., **Gall, M.**, Totu, A., Crunțeanu, D.E., Levențiu, C. (2025) Comparative Study of Noise Control in Micro Turbojet Engines with Chevron and Ejector Nozzles Through Statistical, Acoustic and Imaging Insight. *Applied Sciences*, *15*, 394, https://doi.org/10.3390/app15010394; WOS:001393489200001; ISSN: 2076-3417

III. Publications in BDI journals in the field of PhD thesis

- **Gall, M.**, Dumitrescu, O., Drăgan, V., Gherman, B., & Crunţeanu, D.E. (2023, October). Effects of Perforated Plates on the Performance of Vaned Diffusers for Microgas Turbines. In *2023 11th International Conference on ENERGY and ENVIRONMENT (CIEM)* (pp. 1-5). IEEE, https://doi.org/10.1109/CIEM58573.2023.10349776; ISBN:979-8-3503-4078-5

- **Gall, M.**, Drăgan, V. (2022) Vaned Diffuser Numerical Investigation for Microjet Engine, *Scientific Journal TURBO*, vol. IX (2022), no. 1, *https://comoti.ro/wp-content/uploads/2022/12/11.Scientific-Journal-Turbo-Vol-IX_1_2022.pdf*; ISSN (online): 2559-608X

IV. Projects where the author of the PhD thesis was involved as a team member

- PN-III-CERC-CO-PED-3-2021 PED call for proposals (Experimental Demonstration Programme) by the Executive Agency for Higher Education, Research, Development and Innovation Funding (UEFISCDI) "**Operating range augmentation system through porous walls for centrifugal compressors**", acronym **SPACELESS**, grant no. 717PED/2022

REFERENCES

[1] The European Green Deal, https://commission.europa.eu/strategy-and-policy/priorities-2019-2024/european-green-deal_en accessed on 27th October 2023

[2] Aircraft Micro Turbine Engines Market, https://www.marketsandmarkets.com/Market-Reports/aircraft-micro-turbine-engines-market-248924999.html?gclid=Cj0KCQiArt6PBhCoARIsAMF5wajZnXK2WBYc_RfSzGQcM8xGGVRLkVFl7zRWvYYTpEq3yxxQLhltqZ0aA accessed on 12th February 2022

[3] Marcellan, A. (2015). An exploration into the potential of microturbine based propulsion systems for civil Unmanned Aerial Vehicles, MSc Thesis, TU Delft, Thesis number = 030#15#MT#FPP

[4] Decuypere, R., & Verstraete, D. (2005). Micro turbines from the standpoint of potential users. *VKI LS on micro gas turbines*, Educational Notes RTO-EN-AVT-131, Paper 15, pp. 15-1-15-14, http://myexs.ru/wp-content/uploads/2012/04/EN-AVT-131-15.pdf

[5] Burger, C. J. (2016). *Design procedure of a compact crossover diffuser for micro gas turbine application* (Doctoral dissertation, Stellenbosch: Stellenbosch University), ISSN-L 2310-7855, http://hdl.handle.net/10019.1/98634

[6] Dodge, J. L., Bush, D. B., Pechuzal, G. A., & Ravindranath, A. (1987). High efficiency transonic mixed-flow compressor method and apparatus. *U.S. Patent No. 4,678,398*. Washington, DC: U.S. Patent and Trademark Office

[7] Tiainen, J., Grönman, A., Jaatinen-Värri, A., & Backman, J. (2017). Flow control methods and their applicability in low-Reynolds-number centrifugal compressors—a review. *International Journal of Turbomachinery, Propulsion and Power*, *3*(1), 2, https://doi.org/10.3390/ijtpp3010002

[8] Skoch, G. J. (2005). Experimental investigation of diffuser hub injection to improve centrifugal compressor stability. *J. Turbomach.*, *127*(1), 107-117, https://doi.org/10.1115/1.1812779

[9] Galloway, L., Spence, S., In Kim, S., Rusch, D., Vogel, K., & Hunziker, R. (2018). An investigation of the stability enhancement of a centrifugal compressor stage using a porous throat diffuser. *Journal of Turbomachinery*, *140*(1), 011008, https://doi.org/10.1115/1.4038181

[10] Galloway, L., Rusch, D., Spence, S., Vogel, K., Hunziker, R., & Kim, S. I. (2018). An investigation of centrifugal compressor stability enhancement using a novel vaned diffuser recirculation technique. *Journal of Turbomachinery*, *140*(12), 121009, https://doi.org/10.1115/1.4041601

[11] Malael, I., Bucur, I. O., & Dragan, V. (2020). 2.5 D les simulation of an airfoil shock wave reduction by using porous media. *Aerospace Research in Bulgaria*, *32*, 122-133, https://doi.org/10.3897/arb.v32.e11

[12] Gunasekaran, H., Thangaraj, T., Jana, T., & Kaushik, M. (2020). Effects of wall ventilation on the shock-wave/viscous-layer interactions in a Mach 2.2 intake. *Processes*, *8*(2), 208, https://doi.org/10.3390/pr8020208

[13] Doerffer, P., & Szulc, O. (2007). Shock wave strength reduction by passive control using perforated plates. *Journal of Thermal Science*, *16*, 97-104, https://doi.org/10.1007/s11630-007-0097-z.

[14] Sasoh, A., Matsuoka, K., Nakashio, K., Timofeev, E., Takayama, K., Voinovich, P., ... & Makino, Y. (1998). Attenuation of weak shock waves along pseudo-perforated walls. *Shock Waves*, *8*, 149-159, https://doi.org/10.1007/s001930050108

[15] Lee, B.H.K. (2001) Self-sustained shock oscillations on airfoils at transonic speeds. *Progress in Aerospace Sciences*, 37(2), pp.147-196, https://doi.org/10.1016/S0376-0421(01)00003-3

[16] Raghunathan, S., & Mabey, D. (1986, January). Passive shockwave boundary layer control experiments on a circular arc model. In *24th Aerospace Sciences Meeting* (p. 285), https://doi.org/10.2514/6.1986-285

[17] Roy, S., Sandhu, J. P. S., & Ghosh, S. (2021). Drag reduction in transonic shock-wave/boundary-layer interaction using porous medium: a computational study. *Shock Waves*, *31*(2), 117-132, https://doi.org/10.1007/s00193-021-01009-7

[18] Hamid, M. A., Hasan, A. T., Ali, M., Mitsutake, Y., Setoguchi, T., & Yu, S. (2016). Unsteady transonic flow control around an airfoil in a channel. *Journal of Thermal Science*, *25*, 117-122, https://doi.org/10.1007/s11630-016-0841-3

[19] Doerffer, P., & Szulc, O. (2006). Shock wave smearing by wall perforation. *Archives of Mechanics*, *58*(6), 543-573, https://am.ippt.pan.pl/index.php/am/article/view/228

[20] Raghunathan, S., Gray, J., & Cooper, R. (1987, January). Effect of inclination of holes on passive shock wave boundary layer control. In *25th AIAA Aerospace Sciences Meeting* (p. 437), https://doi.org/10.2514/6.1987-437

[21] Zater, C., Bahi, L. (2024) Passive control of shock wave/turbulent boundary layer interaction using low permeability wall ventilation over a supercritical RAE-2822 airfoil, *Thermophysics and Aeromechanics*, 31, 583–597, https://doi.org/10.1134 /S086986432403020X

[22] Bohning, R., and Doerffer, P. (1995, December) Wind tunnel tests of shock/boundary layer interaction with passive control porous wall investigation and numerical simulation of the wind tunnel tests, *University of Karlsruhe final Report EUROSHOCK TR AER 2-92-49/1.5*

[23] Raghunathan, S. (1987). Effect of porosity strength on passive shock-wave/boundary-layer control. *AIAA journal*, *25*(5), 757-758, https://doi.org/10.2514/3.9693

[24] Egon, S., Delery, J., Fulker, J., Wolfgang, G. (1997) EUROSHOCK—Drag reduction by Passive Shock Control, *Results of the Project EUROSHOCK*, AER2-CT92-0049 Supported by the European Union, 1993–1995; European Union: Brussels, Belgium, 1997; Volume 56, ISBN 978-3-322-90713-4

[25] Savu, G. (1983). Suppression of shocks on transonic airfoils. In *14th International Symposium on Shock Tube and Wave*, Sydney, Australia, pp. 92-101

[26] Szulc, O., Doerffer, P., Flaszynski, P., & Suresh, T. (2020). Numerical modelling of shock wave-boundary layer interaction control by passive wall ventilation. *Computers & Fluids*, *200*, 104435, ISSN 0045-7930, https://doi.org/10.1016/j.compfluid.2020.104435

[27] **Gall, M.**, Drăgan, V. (2022) VANED DIFFUSER NUMERICAL INVESTIGATION FOR MICROJET ENGINE, *Scientific Journal TURBO*, vol. IX (2022), no. 1, *https://comoti.ro/wp-content/uploads/2022/12/11.Scientific-Journal-Turbo-Vol-IX_1_2022.pdf*

[28] **Gall, M.**, Dumitrescu, O., Drăgan, V., Gherman, B., & Crunţeanu, D. E. (2023, October). Effects of Perforated Plates on the Performance of Vaned Diffusers for Microgas Turbines. In *2023 11th International Conference on ENERGY and ENVIRONMENT (CIEM)* (pp. 1-5). IEEE, https://doi.org/10.1109/CIEM58573.2023.10349776

[29] **Gall, M.**, Dumitrescu, O., Drăgan, V., & Crunțeanu, D. E. (2024). Effects of Perforated Plates on Shock Structure Alteration for NACA0012 Airfoils. *Inventions*, *9*(2), 28, https://doi.org/10.3390/inventions9020028

[30] **Gall, M.**, Dumitrescu, O., Drăgan, V., & Crunțeanu, D. E. (2024). Effects of Perforated Plates on Shock Structure Alteration for NACA0012 Cascade Configurations. *Inventions*, *9*(5), 110, https://doi.org/10.3390/inventions9050110

[31] Dumitrescu, O., **Gall, M.**, & Drăgan, V. (2023). A Three-Dimensional Design to Study the Shock Waves of Linear Cascade with Reduced Mass Flow Requirements. *Applied Sciences*, *13*(19), 11029, https://doi.org/10.3390/app131911029

[32] **Gall, M.**, Drăgan, V., Dumitrescu, O., Prisăcariu, E. G., Condruz, M. R., Paraschiv, A., Petrescu, V., & Vlăduț, M. (2024). Design, Fabrication, and Commissioning of Transonic Linear Cascade for Micro-Shock Wave Analysis. *Journal of Manufacturing and Materials Processing*, *8*(5), 201, https://doi.org/10.3390/jmmp8050201

[33] Drăgan, V., Dumitrescu, O., **Gall, M.**, Prisăcariu, E. G., & Gherman, B. (2024). Experimental Identification of a New Secondary Wave Pattern in Transonic Cascades with Porous Walls. *Aerospace*, *11*(11), 946, https://doi.org/10.3390/aerospace11110946

[34] Cican, G., **Gall, M.**, Bogoi, A., Deaconu, M., & Crunțeanu, D. E. (2023). Experimental Investigation of a Micro Turbojet Engine Chevrons Nozzle by Means of the Schlieren Technique. *Inventions*, *8*(6), 145, https://doi.org/10.3390/inventions8060145

[35] Bogoi, A., Cican, G., **Gall, M.**, Totu, A., Crunțeanu, D. E., & Levențiu, C. (2025). Comparative Study of Noise Control in Micro Turbojet Engines with Chevron and Ejector Nozzles Through Statistical, Acoustic and Imaging Insight. *Applied Sciences*, *15*(1), 394, https://doi.org/10.3390/app15010394

[36] Dumitrescu, O., et al., Technical Report COMOTI, Project 717PED contract 'Operating range augmentation system through porous walls for centrifugal compressors – SPACELESS', Etapa I. Fabricatie compresor centrifugal - Faza 1. Campanie experimentala - Faza 1, P.V.A. nr. 89/24.11.2022

[37] Dumitrescu, O., et al., Technical Report COMOTI, Project 717PED contract 'Operating range augmentation system through porous walls for centrifugal compressors – SPACELESS', Etapa II. Fabricatie compresor centrifugal - Faza 2. Campanie experimentala - Faza 2. Diseminarea rezultatelor - Faza 1, P.V.A. nr. 74/27.11.2023

[38] Dumitrescu, O., et al., Technical Report COMOTI, Project 717PED contract 'Operating range augmentation system through porous walls for centrifugal compressors – SPACELESS', Etapa III. Campanie experimentala - Faza 3. Diseminarea rezultatelor - Faza 2, P.V.A. nr. 29/13.06.2024